JVI Journals.ASM.org

Complementary Induction of Immunogenic Cell Death by Oncolytic Parvovirus H-1PV and Gemcitabine in Pancreatic Cancer

Assia L. Angelova,[a] Svitlana P. Grekova,[a] Anette Heller,[b] Olga Kuhlmann,[a] Esther Soyka,[b] Thomas Giese,[c] Marc Aprahamian,[d] Gaétan Bour,[d] Sven Rüffer,[b] Celina Cziepluch,[a] Laurent Daeffler,[a] Jean Rommelaere,[a] Jens Werner,[b] Zahari Raykov,[a] Nathalia A. Giese[b]

Programme Infection and Cancer, Tumour Virology Division F010, German Cancer Research Center (DKFZ), Heidelberg, Germany[a]; Department of General Surgery, University Hospital Heidelberg, Heidelberg, Germany[b]; Institute of Immunology, University Hospital Heidelberg, Heidelberg, Germany[c]; Institut de Recherche contre les Cancers de l'Appareil Digestif (IRCAD), Strasbourg, France[d]

ABSTRACT

Novel therapies employing oncolytic viruses have emerged as promising anticancer modalities. The cure of particularly aggressive malignancies requires induction of immunogenic cell death (ICD), coupling oncolysis with immune responses via calreticulin, ATP, and high-mobility group box protein B1 (HMGB1) release from dying tumor cells. The present study shows that in human pancreatic cancer cells (pancreatic ductal adenocarcinoma [PDAC] cells; $n = 4$), oncolytic parvovirus H-1 (H-1PV) activated multiple interconnected death pathways but failed to induce calreticulin exposure or ATP release. In contrast, H-1PV elevated extracellular HMGB1 levels by 4.0 ± 0.5 times (58% ± 9% of total content; up to 100 ng/ml) in all infected cultures, whether nondying, necrotic, or apoptotic. An alternative secretory route allowed H-1PV to overcome the failure of gemcitabine to trigger HMGB1 release, without impeding cytotoxicity or other ICD activities of the standard PDAC medication. Such broad resistance of H-1PV-induced HMGB1 release to apoptotic blockage coincided with but was uncoupled from an autocrine interleukin-1β (IL-1β) loop. That and the pattern of viral determinants maintained in gemcitabine-treated cells suggested the activation of an inflammasome/caspase 1 (CASP1) platform alongside DNA detachment and/or nuclear exclusion of HMGB1 during early stages of the viral life cycle. We concluded that H-1PV infection of PDAC cells is signaled through secretion of the alarmin HMGB1 and, besides its own oncolytic effect, might convert drug-induced apoptosis into an ICD process. A transient arrest of cells in the cyclin A1-rich S phase would suffice to support compatibility of proliferation-dependent H-1PV with cytotoxic regimens. These properties warrant incorporation of the oncolytic virus H-1PV, which is not pathogenic in humans, into multimodal anticancer treatments.

IMPORTANCE

The current therapeutic concepts targeting aggressive malignancies require an induction of immunogenic cell death characterized by exposure of calreticulin (CRT) as well as release of ATP and HMGB1 from dying cells. In pancreatic tumor cells (PDAC cells) infected with the oncolytic parvovirus H-1PV, only HMGB1 was released by all infected cells, whether nondying, necrotic, or succumbing to one of the programmed death pathways, including contraproductive apoptosis. Our data suggest that active secretion of HMGB1 from PDAC cells is a sentinel reaction emerging during early stages of the viral life cycle, irrespective of cell death, that is compatible with and complements cytotoxic regimens. Consistent induction of HMGB1 secretion raised the possibility that this reaction might be a general "alarming" phenomenon characteristic of H-1PV's interaction with the host cell; release of IL-1β points to the possible involvement of a danger-sensing inflammasome platform. Both provide a basis for further virus-oriented studies.

Pancreatic ductal adenocarcinoma (PDAC) is an extremely aggressive disease, with a median survival time of less than 9 months and a 5-year survival rate of <1%. Current advances in surgical, (neo)adjuvant, and palliative treatments have failed to prevent recurrence and ultimate metastasis (1–3).

In order to be effective, chemotherapy must reduce the tumor burden, promote anticancer immunity, and alleviate intratumoral immunosuppression (4–6). Forced tumor cell death in an immunogenic manner (i.e., immunogenic cell death [ICD]) has been proposed as the best way to trigger an adaptive immune response, boosting the therapeutic efficacy of a cytoreductive treatment (7, 8). Preapoptotic surface exposure of calreticulin (CRT) (as a result of the endoplasmic reticulum stress response), as well as release of ATP (autophagy) and high-mobility group box B1 protein (HMGB1) (late apoptosis/necrosis), is considered the optimal ICD combination for dying tumor cells to enable paracrine activation of dendritic cells and the consequent priming of cytotoxic effectors. The surface exposure of CRT promotes uptake of dying tumor cells by dendritic cells, and the release of HMGB1 engages

Received 28 January 2014 Accepted 17 February 2014
Published ahead of print 26 February 2014
Editor: G. McFadden
Address correspondence to Nathalia A. Giese, nathalia.giese@med.uni-heidelberg.de.
A.L.A., S.P.G., and A.H. contributed equally to this article.
Supplemental material for this article may be found at http://dx.doi.org/10.1128/JVI.03688-13.

doi:10.1128/JVI.03688-13

Toll-like receptor 2 (TLR2)/TLR4/RAGE-mediated signaling, whereas secretion of ATP initiates P2X7-mediated activation of the inflammasome and caspase 1 (CASP1), marked by the processing and production of matured interleukin-1β (IL-1β) (9). Although not universal, induction of this triad has been proven to underlie the success of chemotherapy in various transplantable and carcinogen-induced mouse tumor models, as well as in humans (10–14). ICD induces sustained anticancer protection; however, only a few cytotoxic agents fulfil all the aforementioned ICD requirements, meaning that specific supplements are required (15).

The nucleoside analogue gemcitabine (GEM) (Gemzar; Eli Lilly, Indianapolis, IN)—the only cytotoxic drug approved for the standard treatment of PDAC—exerts an array of immune modulatory effects and improves the outcomes of antitumor vaccination approaches (16–20). However, while the use of gemcitabine as a single agent or as a principal component of multimodal approaches has shown clear clinical benefits, there has been no long-term protection thus far (21).

Novel therapies employing oncolytic viruses have emerged as promising anticancer modalities (22). The autonomous parvoviruses H-1PV and prototype strain of the minute virus of mice MVMp are rarely virulent in their natural adult hosts but possess the ability to infect, propagate in, and kill transformed cells (23–25). Over the past years, different preclinical models have been used to demonstrate that the rodent parvovirus H-1PV—which displays oncotropism, lack of preexisting antiviral immunity, and good safety records—might be used to treat human malignancies (26–28). Experiments with melanoma and glioma cells showed that H-1PV-induced tumor cell death promotes phagocytosis, maturation, cross-presentation by dendritic cells, and cytotoxic T-cell activation and that these effects are promotable by the chemotherapeutics cisplatin, vincristine, and sunitinib (29–31). H-1PV is highly efficient in eliminating PDAC cells, and its action is greatly enhanced by gemcitabine (32, 33). The combination of *in vitro* experiments, studies in immunodeficient mice with human xenografts, and studies in immunocompetent rat models showed that the anticancer protection comprises cytoreductive and immune-mediated components, with gamma interferon (IFN-γ) emerging as a critical end effector (34–36). Yet the mechanism underlying the induction of the immune reaction remains obscure.

The release of ICD determinants upon infections in general, and by tumor cells infected with oncolytic viruses in particular, has started to draw attention (37–43). We hypothesized that triggering the adaptive anticancer activity by H-1PV—alone or in combination with gemcitabine—could be initiated by ICD determinants released from dying tumor cells. The aim of the current study was to establish whether (i) H-1PV might induce oncolysis in PDAC cells; (ii) the cell death mode is immunogenic, i.e., promotes emanation of CRT, ATP, and HMGB1; and (iii) H-1PV-induced ICD is compatible with the major anti-PDAC chemotherapeutic, GEM.

MATERIALS AND METHODS

During this study, we used well-established methods as detailed previously (32, 44).

H-1PV production and titration. Wild-type H-1PV to be used for infection of PDAC cells was produced by infecting NBK cells and purifying released virions by using iodixanol gradient centrifugation and dialysis against Ringer solution. Virus titers were measured by standard plaque assays and expressed as numbers of PFU per ml. Virus stock contamination with endotoxin was less than 2.5 endotoxin units (EU)/ml.

Cell cultures and treatments. The panel of studied PDAC-derived cell lines included AsPC1, MiaPaca2, Panc1, and T3M4 cells. The identities of the cells were certified by the DSMZ. The cells were routinely grown in RPMI 1640 medium (Sigma, Hamburg, Germany) supplemented with 10% fetal bovine serum, 100 U/ml penicillin, and 100 μg/ml streptomycin. The PDAC cells were seeded as triplicates at 2×10^3 cells/100 μl in 96-well plates, 2×10^4 cells/ml in 24-well plates, 1×10^5 cells/2 ml in 6-well plates, or 1×10^6 to 2×10^6 cells/10 ml in 10-cm petri dishes (Nunclon; Thermo Fischer Scientific GmbH, Dreieich, Germany). On the next day, the cells were exposed to H-1PV at multiplicities of infection (MOIs) of 10 to 50 PFU/cell, with or without previous exposure to the anti-PDAC chemotherapeutic gemcitabine (GEM) (Gemzar; Eli Lilly & Co., Indianapolis, IN) for 0 to 12 h. GEM was tested at doses ranging from the 50% inhibitory concentrations (IC_{50}s) (9, 8, 400, and 1.2 ng/ml, i.e., 4 nM to 1.3 μM) to 100× IC_{50} (32) or 40 ng/ml (133 nM) to cause an H-1PV-like level of oncolysis; these data were combined for the final presentation. Cells and supernatants were collected at assay-specific time points between 1 and 72 h posttreatment (hpt) and assayed as described below. The chemical compounds used to elucidate the contributions of different death pathways in infected PDAC cultures and their working concentrations (with their own cytotoxicities of <15%) are listed in Table 1.

siRNA-based CRT knockdowns. Cells were grown in 6-well plates and transfected with commercially available Silencer Select validated small interfering RNA (siRNA) sense-antisense sets by use of Hiperfect. The reduction of CRT protein levels was achieved by 5 nM CRT sets 4390824/s114 (si1) and 4390824/s115 (si2). As a control, we used a Silencer negative-control siRNA (AM4635; nc-si) (all from Ambion). Forty-eight hours later, cells were harvested and analyzed for CRT protein expression by Western blotting and fluorescence-activated cell sorter (FACS) analyses.

Cell viability and cytotoxicity assays. The cellularity of infected PDAC cultures was assessed at 72 hpt by standard crystal violet staining (CVS) of viable cells. The images of stained monolayers were recorded using a Leica DM IL inverted microscope (Leica, Bensheim, Germany). Quantification of growth was achieved by dissolving the incorporated dye with methanol and measuring the optical density at 595 nm (OD_{595}) using a Multiscan EX reader (Thermo Fisher Scientific). The values for infected cultures were compared to those for noninfected cultures and expressed as percentages of mock sample values (% of mock). The cytotoxicity of the treatments (oncolysis) was assessed by simultaneous measurement of lactate dehydrogenase (LDH), leaked from the cells into the growth medium, using a commercially available colorimetric CytoTox 96 nonradioactive cytotoxicity assay from Promega (Madison, WI). The absorbance values for supernatants were related to the maximum amount of LDH in the cultures (total lysis with 0.8% Triton X-100) and expressed as percentages of total content to estimate the degree of lysis. Detection of LDH release provides an easy method for determining the extent of cell death, irrespective of the type of cell death (45, 46).

Analysis of released ICD determinants. The concentrations of the proteins in the culture supernatants were measured using a commercially available CellTiter-Glo Luminescent assay for ATP (Promega, Madison, Wisconsin, USA) and enzyme-linked immunosorbent assay (ELISA) kits from eBioscience for IL-1β (Frankfurt, Germany) and from Shino-Test Corporation for HMGB1 (Kanagawa, Japan).

FACS analysis. FACS analysis was used to determine expression of ICD determinants on the surfaces of treated cells, as well as to monitor cell cycle and apoptotic changes caused by treatments in PDAC cells. H-1PV-exposed PDAC monolayers, with or without GEM treatment, were harvested using 1 mM EDTA–phosphate-buffered saline (PBS) detachment buffer, blocked (Miltenyi GmbH, Bergisch Gladbach, Germany), and incubated for 45 min on ice with isotype IgG controls, anti-HSP70 (Santa

TABLE 1 Chemicals used to inhibit specific death pathways in H-1PV-infected PDAC cells

Inhibitor	Source	Specific process/target	Mechanism of action and specific intracellular effects	Effective dose range	Dose used
Z-VAD-FMK	R&D Systems	Apoptosis (pan-caspases)	Cell permeative, irreversibly binds to caspases' catalytic sites; caspase inactivation might cause a shift toward necrosis	50 nM–100 μM	10 μM
3-MA	Sigma	Autophagy	Cell-permeating autophagic sequestration blocker; class III phosphatidylinositol 3-kinase (PI3K) inhibitor	5–10 mM	1 mM
Ac-LVK-CHO	Calbiochem	Cathepsin B	Water-soluble cathepsin B inhibitor	10–50 nM	50 nM
CA-074 Me	Sigma	Cathepsin B	Cell-permeating, irreversible, selective cathepsin B inhibitor; activity depends on intracellular esterases	1–10 μM	1 μM
Z-FL-COCHO	Calbiochem	Cathepsin S	Slow, tight-binding, reversible inhibitor of cathepsin S	1–2 nM	1 μM
IM-54	Calbiochem	Oxidative stress-induced necrosis	Cell-permeating selective inhibitor of H_2O_2-induced necrosis; does not display antioxidant properties	1–10 μM	10 μM
Necrostatin-1	Sigma	Necroptosis (RIP1 kinase)	Inhibits RIP1 kinase and nonapoptotic cell death; inhibits MMP in TNF-α-treated Jurkat cells	20–300 μM	20 μM

Cruz Biotechnologies), anti-CD47 (Immunotools, Germany), or a panel of five anti-CRT antibodies: (i) rabbit IgG (ab2907), (ii) mouse IgG1 clone FMC75 (ab22683), (iii) FMC75-phycoerythrin (PE) (ab83220) (all from Abcam, Cambridge, MA), (iv) mouse IgG2bk-fluorescein isothiocyanate (FITC) (3730-7) (Mabtech, Cincinnati, OH), and (v) rabbit IgG-AF488 (bs-5913R-AF488) (Bioss Inc., Woburn, MA). Goat anti-rabbit IgG–DyLight488 (KPL, Gaithersburg, MD), goat anti-mouse IgG1–AF488 (Life Technologies GmBH, Darmstadt, Germany), and goat anti-mouse IgG(H+L)–FITC (Jackson Immunoresearch Lab Inc., West Grove, PA) were subsequently applied to nonlabeled rabbit and mouse antibodies. As a positive control for CRT, we performed treatment of PDAC cells with 1 μM cytostatic anthracenedione mitoxantrone (MTX; Sigma-Aldrich Chemie GmbH, Taufkirchen, Germany). Annexin V-propidium iodide (AnnV-PI) expression was measured using an AnnexinV-FLUOS staining kit (Roche Applied Science [RAS], Mannheim, Germany) according to the manufacturer's instructions. Samples were analyzed with a FACSCalibur flow cytometer using CellQuest software (Becton, Dickinson, San Jose, CA). The cell cycle was analyzed using a Guava cell cycle reagent and instrument (Merck Millipore, Merck KGaA, Darmstadt, Germany).

Immunofluorescence detection of infected cells. The newly synthesized nonstructural protein NS1 of H-1PV was visualized using cells grown on glass coverslips overnight (Menzel GmbH, Braunschweig, Germany) and infected with H-1PV at an MOI of 10 PFU/cell. At 48 hpt, cells were fixed and permeabilized using 4% paraformaldehyde and 0.2% Triton X-100–PBS solutions. After blocking with 1% normal donkey serum, cells were stained with the mouse NS1-specific monoclonal antibody 3D9 (a gift from Nathalie Salomé, DKFZ, Heidelberg, Germany) at a 1:50 dilution in 1% bovine serum albumin (BSA)-PBS for 1 h at room temperature. Following subsequent exposure with the secondary antibody in the form of Alexa Fluor 594-labeled donkey anti-mouse IgG (1:400 in BSA-PBS) (Molecular Probes, Eugene, OR) for 1 h, the cells were mounted with Vectashield medium containing DAPI (4′,6-diamidino-2-phenylindole) (Vector Laboratories, Burlingame, CA). Immunofluorescence was recorded using a Leica DMRBE fluorescence microscope (Leica, Bensheim, Germany), and the number of NS1-positive cells was counted manually.

Real-time qRT-PCR and Western blotting. The expression of viral (NS1) and cellular (HMGB1, IL-1β, and cyclophilin B) mRNA was analyzed using a commercially available mRNA MagNA Pure LC HS isolation kit, a cDNA synthesis kit, and PCR reagents and primers for a LightCycler480 instrument, delivered by RAS (Mannheim, Germany) and Search-LC (Heidelberg, Germany). The transcript numbers for NS1, HMGB1, and IL1-β were normalized to 10,000 copies of the housekeeping gene cyclophilin B (10 kCPB). The viral DNA (vDNA) versus mRNA specificity of NS1 quantitative reverse transcriptase PCR (qRT-PCR) was controlled in each individual sample by performing NS1 PCR with samples in which reverse transcriptase was omitted during the cDNA synthesis step ($cDNA^{RT-}$). Although the mRNA isolation procedure included a treatment with DNase, our final $cDNA^{RT+}$ samples contained 3.0% ± 0.03% residual viral DNA (according to NS1 levels in $cDNA^{RT-}$ compared to $cDNA^{RT+}$ samples). Visualization of the PCR products obtained from $cDNA^{RT-}$ samples by means of agarose gel electrophoresis confirmed the amplification of a 512-bp vDNA-derived fragment. This contaminating vDNA band, however, was not seen in $cDNA^{RT+}$ samples, which displayed a 415-bp product derived from the major spliced transcript. Such a pattern indicated that the utilized qRT-PCR conditions exclusively amplified the abundant $cDNA^{RT+}$ template. Mock- and GEM-treated PDAC cultures served as negative controls (no signal was detected).

The expression of viral and cellular proteins was analyzed by Western blotting. RIPA buffer-lysed cells were analyzed for H-1PV nonstructural (NS1-NS2) and structural (capsid VP1 to VP3) proteins as well as for cellular full and cleaved forms of caspase 3 (CASP3), PARP1, HMGB1 (Shino-Test Corp., Kanagawa, Japan), and β-actin. Upon chemiluminescence visualization, the band intensities were quantified using ImageJ software (NIH-NCBI, Bethesda, MD), normalized to β-actin values, and expressed as percentages of respective control levels.

Viral DNA replication and production. Viral DNA replicative forms were detected by Southern blotting as described previously (47). In short, H-1PV DNA isolated by the Hirt method was fractionated by 0.8% agarose gel electrophoresis and visualized by Southern blotting upon transfer of DNA to a Hybond-N nitrocellulose membrane (Amersham GmbH, Freiburg, Germany) and hybridization to a ^{32}P-labeled H-1PV DNA-specific probe. The DNA bands reflecting accumulation of viral replicative intermediates, i.e., single-stranded DNA (ssDNA), the converted double-stranded monomeric form (mRF), and the dimeric double-stranded form (dRF), were recorded at 24, 48, and 72 hpt.

The amounts of infectious particles released by the cells at 72 hpt were determined with an infectious center assay (ICA) using sensitive NBK cells.

Intracellular distribution of CTSB and CTSS. PDAC cells were plated at a density of 1×10^6 in 10-cm petri dishes overnight, infected at an MOI of 10 PFU/cell, and harvested at 48 hpt to determine changes in intracellular distribution of cathepsin B and S (CTSB and CTSS) activities (48).

CTSB and CTSS activities were measured in the cytosolic and crude lysosomal fractions by using the fluorogenic CTSB substrate Z-Arg-Arg-AMC (EMD Millipore, Billerica, MA) at a final concentration of 1 mM and the CTSS substrate Ac-Lys-Gln-Lys-Leu-Arg-AMC (AnaSpec, San Jose, CA) at a final concentration of 200 μM. The reaction was monitored on a Fluoroskan Ascent FL instrument (Thermo) for 1 h at 360 and 455 nm, for excitation and emission, respectively. Data are presented as the ratios between enzymatic activities in the cytosolic versus lysosomal fractions.

Statistical analyses. GraphPad Prism5 (GraphPad Software, Inc., La Jolla, CA) was used to analyze and present the data obtained from experiments repeated two to eight times for each cell line. The figures summarize the findings and show means ± standard errors of the means (SEM) for each group, with the differences considered significant at P values of <0.05, as determined by paired Wilcoxon test, two-way analysis of variance (ANOVA), or the Kruskal-Wallis test with the Dunn test.

RESULTS

H-1PV infection of PDAC cells triggers release of HMGB1 but not CRT or ATP. In order to determine the immunogenic profile of H-1PV-infected PDAC cells ($PDAC^{H\text{-}1PV}$), a panel of four cell lines (AsPC1, MiaPaca2, Panc1, and T3M4) was infected with H-1PV at an MOI of 10 PFU/cell and analyzed for expression of the ICD determinants CRT, ATP, and HMGB1 at 4, 12, 24, 48, and 72 hpt. This treatment promoted release of HMGB1 but not ATP, CRT (Fig. 1A to C), or other ICD determinants known to facilitate or inhibit immunogenicity of dying cells (heat shock protein HSP70, uric acid, or CD47) (data not shown).

The induction of HMGB1 release emerged as a strikingly robust feature of H-1PV, with the supernatants of $PDAC^{H\text{-}1PV}$ cultures containing 4.0 ± 0.5 times more protein than the mock-infected ones (2-way ANOVA; $P = 0.008$) (Fig. 1A). Extracellular HMGB1 rose continuously and reached 30 to 100 ng/ml 72 h after infection of 2×10^4 cells, accounting for 58% ± 9% of total HMGB1 content, compared to less than 10% in noninfected cultures.

The lack of CRT translocation to the surface—despite high intracellular levels and mitoxantrone-induced control exposure (Fig. 1D and E)—was proved by means of five anti-CRT antibodies. It should be mentioned that none, other than the phycoerythrin-conjugated mouse FMC75 clone (FMC75-PE; Abcam), detected constitutive CRT expression. This antibody stained noninfected MiaPaca2 and T3M4 cells (Fig. 1F), suggesting the constitutive expression of CRT on the surface in 2 of 4 PDAC cell lines. Yet siRNA-based CRT knockdowns did not alter the FACS positivity of the FMC75-PE antibody (Fig. 1G), although these treatments reduced expression of the CRT protein detectable by Western blotting with all used antibodies, including unlabeled FMC75 and PE-conjugated clones (Fig. 1H and I). This pattern implied cross-reactivity of the frequently used PE conjugate with a surficial non-CRT target and indicated that FMC75-PE-based observations (current or previously published) should be interpreted with extreme caution.

Induction of death by H-1PV in PDAC cells. The HMGB1-biased pancreatic ICD profile suggested preferential activation of a distinct death pathway. CRT translocation is believed to require proapoptotic redox/ER stress, while ATP release is associated with autophagy. In contrast, HMGB1 production reflects passive, damage-associated necrosis, with apoptosis being contraproductive (10). H-1PV was shown to activate various oncolytic modalities in human tumor cells (26, 48–53). To assess cytoreduction in $PDAC^{H\text{-}1PV}$ cultures, we combined two assays, i.e., crystal violet staining (CVS) of surviving cells and assay of LDH release from lysed cells, and performed annexin V-propidium iodide (AnnV-PI)-based FACS analyses to discriminate between apoptosis and necrosis.

At an MOI of 10 PFU/cell, H-1PV infected 30% to 80% of the PDAC cell population and reduced cellularity by 7% to 63%, with 6% to 40% of the culture being lysed by 72 hpt (Fig. 2A and B). Surprisingly, infectivity did not always determine a cytotoxic outcome. Concordance of these parameters in MiaPaca2 and T3M4 cells was contrasted by death resistance of similar (AsPC1 cells) or highly efficient (Panc1 cells) infected variants. On average ($n = 4$ cell lines), H-1PV infected 52% ± 10% of the PDAC cell population and reduced the total number of cells to 70% ± 12% of the original number. Of those, 27% ± 7% were moribund and underwent oncolysis, reducing the mean survival rate to 53% ± 13%. At an MOI of 50 PFU/cell, the cytoreductive values reached 66% ± 7%, 52% ± 12%, and 32% ± 10%, respectively (Fig. 2C and D).

The AnnV-PI staining pattern revealed that accidental necrosis was not the primary death modality. Only a few $PDAC^{H\text{-}1PV}$ cells displayed the distinct necrotic $AnnV^-$ PI^+ phenotype characterizing primary lytic disintegration (Fig. 2E). Much more frequently, PI positivity coincided with AnnV positivity. Such an $AnnV^+$ PI^+ phenotype revealed a loss of integrity with still-present cellular membranes, which is a hallmark of programmed death processes ranging from primary (pyroptosis or necroptosis) to secondary (postapoptotic) necrosis (46, 54–60). Transient increases in membrane permeability might also occur in association with nonlethal pore opening (61). Accumulation of cells with an apoptotic $AnnV^+$ (PI^-) phenotype, reflecting early externalization of phosphatidylserine in the absence of increased membrane permeability, was observed in infected MiaPaca2 and T3M4 cultures. Induction of apoptosis was further confirmed by Western blotting, showing characteristic cleavage of CASP3 and PARP1 only in these susceptible cell lines, not in AsPC1 and Panc1 cells (Fig. 2F). Together, the CVS, LDH, and FACS data implied that in $PDAC^{H\text{-}1PV}$ cells, necrotic loss of membrane integrity was common but induced differently, and it coincided with HMGB1 release under nonlethal, nonapoptotic, and apoptotic conditions.

Intertwined death pathways in $PDAC^{H\text{-}1PV}$ cells. To determine the mode of cell death in $PDAC^{H\text{-}1PV}$ cells, we sought to determine which specific pathway should be inhibited in order to prohibit infected cells from dying (Table 1). As shown in Fig. 2G and H, none of the inhibitors tested restored viability of the PDAC cultures infected at an MOI of 50 PFU/cell. Only necrostatin-1, an antinecroptotic agent, partially reduced LDH release, and that exclusively in T3M4 cells. In contrast, application of IM-54 (oxidative stress), Z-VAD-FMK (apoptotic and pyroptotic caspases), and 3-MA (autophagy) not only failed to restore cellularity of $PDAC^{H\text{-}1PV}$ cultures but also strongly promoted LDH release. We observed common increases of 10% to 50% in IM-54-treated cells, concurring with 25 to 50% increases in Z-VAD-FMK-treated Panc1 or T3M4 cells and with a 20% gain in 3-MA-treated MiaPaca2 or T3M4 cells. These results indicated concomitant activation of the oxidative stress and other death pathways in $PDAC^{H\text{-}1PV}$ cells, whose blockade most probably altered the killing mode in the infected cell. We suspect that early protective blocking lethality could promote viral production and microtubular changes in initially "rescued" cells, possibly facilitating "collateral" leakage of LDH via transient pore opening during viral egress (61–64).

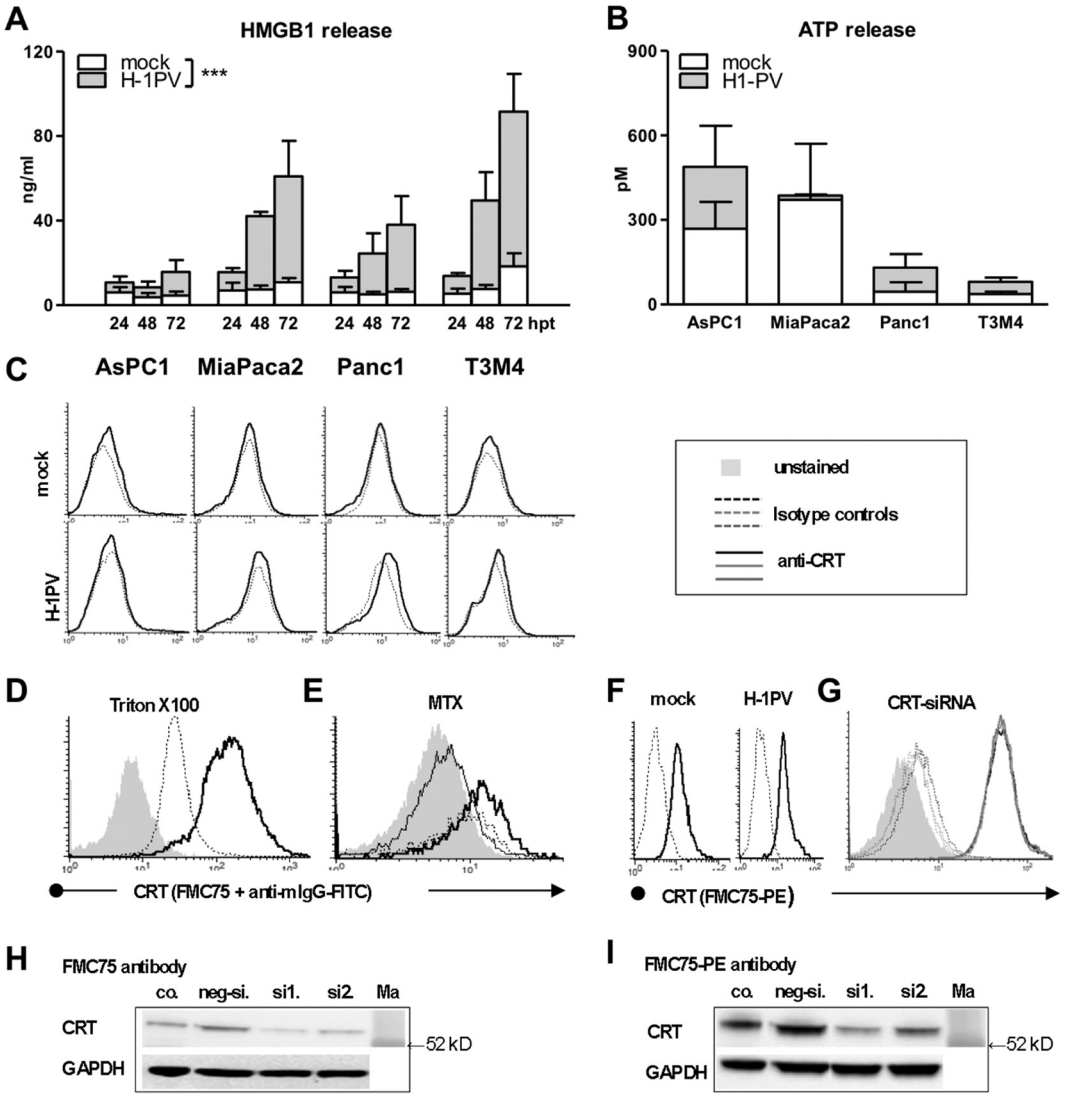

FIG 1 Selective induction of HMGB1 but not CRT or ATP response by oncolytic parvovirus H-1PV in PDAC cells. The pancreatic cancer cell lines AsPC1, MiaPaca2, Panc1, and T3M4 were treated with H-1PV at an MOI of 10 PFU/cell. Cells and supernatants were harvested between 0 and 72 hpt. (A) H-1PV triggered extracellular HMGB1 accumulation as determined by ELISA analysis of supernatants (significant difference between mock- and virus-infected cultures as determined by two-way ANOVA; ***, $P < 0.001$). H-1PV failed to trigger ATP release (ELISA analysis of supernatants at 48 h) (B) and calreticulin exposure (FACS analyses of the cells at 24 h) (dotted lines depict staining with an isotype IgG control, and bold black lines depict staining with anti-CRT antibody) (C). Data shown were obtained with a mouse monoclonal anti-human CRT antibody (clone FMC75) and a subsequently added goat anti-mouse IgG–FITC conjugate. (D to I) A set of confirmatory experiments demonstrated the ability of anti-CRT antibody to detect intracellular CRT in Triton X-100-treated cells (Panc1 cells) (D) and surficial CRT in mitoxantrone (MTX)-treated cells (MiaPaca2 cells; bold black line in comparison to dotted line depicting MTX isotype control and to thin black line depicting overlapping isotype IgG and CRT staining in nontreated cells) (E). The inability of H-1PV to induce CRT exposure was demonstrated by a panel of five antibodies, although one antibody, a directly labeled FMC75 conjugate (ab22683; Abcam), suggested constitutive positivity of MiaPaca2 (F) and T3M4 (not shown) cells, which, however, were not susceptible to siRNA-based CRT knockdown (G). The histograms for siRNA-silenced cells (negative siRNA [neg-si.] and CRT siRNA sets 1 and 2 [si1. and si2.]) are shown as dotted lines for staining with isotype IgG control and as bold lines for staining with anti-CRT antibody. Although Western blot analysis of CRT knockdowns confirmed CRT binding of all antibodies, including the unlabeled FMC75 clone (H) and the FMC75-PE conjugate (I), retention of the CRT-FACS profile suggested additional off-target activity of the latter. co., control; Ma, marker.

Oxidative stress can cause lysosomal disruption and release of proteases into the cytosol (65). Translocation of the cathepsins to the cytosol might represent a marker and/or effector of necrotic cell death. As H-1PV was described to destabilize lysosomal membranes, we additionally checked whether cytoplasmic activation of the cathepsins might contribute to mortality of infected cells. In comparison to mock-infected cells, the ratio between cytosolic and lysosomal activities of cathepsins B and S (CTSB and -S) rose by 2 (AsPC1 cells), 10 (MiaPaca2 and Panc1 cells), and 40 (T3M4 cells) times upon infection (mean, 16 ± 8 times) (Fig. 2I). Nevertheless, exposure of infected cells to the CTSB inhibitors Ac-LVK-CHO and CA-074Me (Fig. 2G and H), as well as the CTSS inhibitor Z-FL-COCHO (not shown), failed to restore cellularity or prevent oncolysis. These data indicated that intracellular liberation of cathepsins revealed increased permeability of the lysosomal membranes but was not an effector of oncolysis in $PDAC^{H\text{-}1PV}$ cells.

All in all, H-1PV infection activated various intertwined death

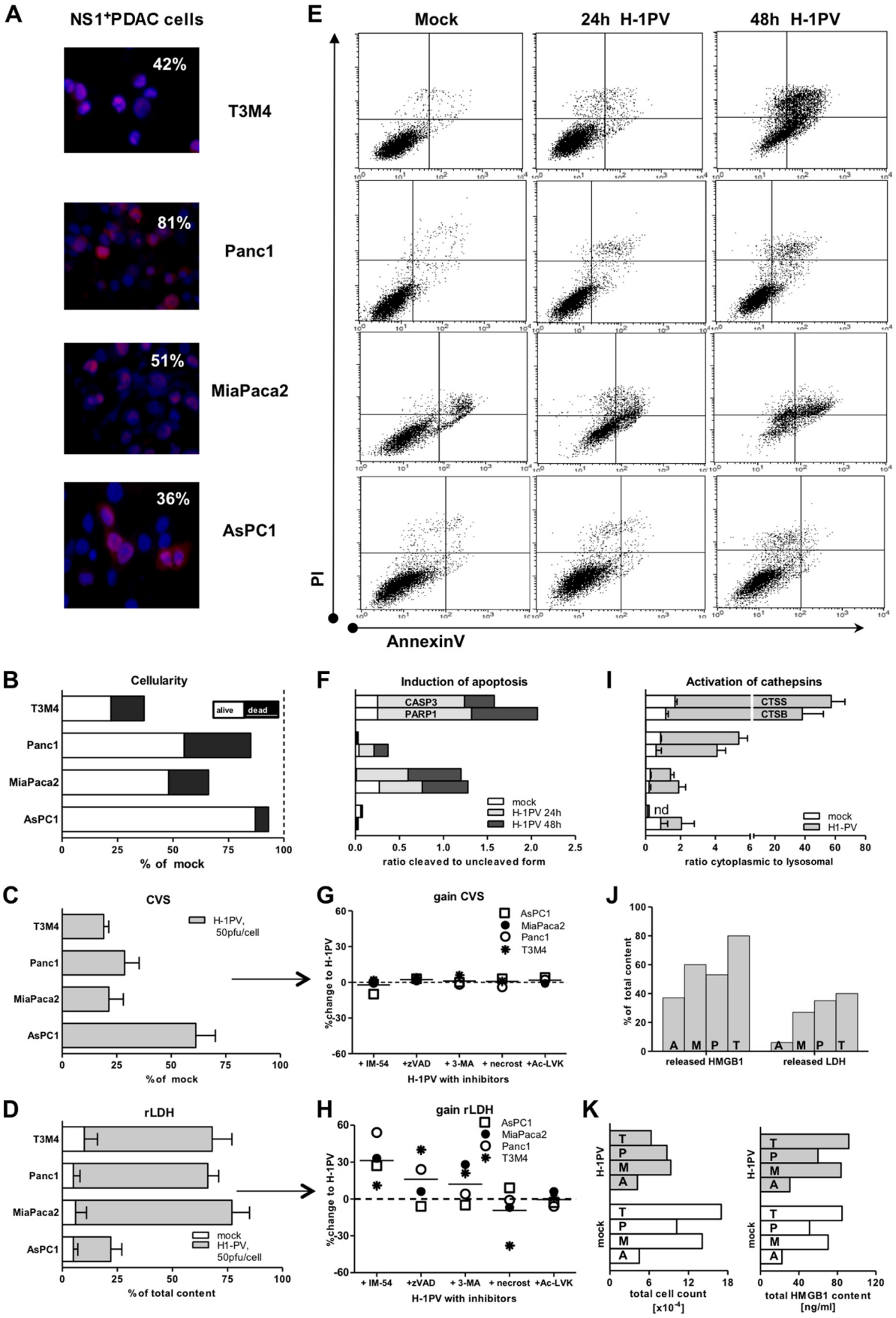
A
NS1+PDAC cells
42%
T3M4
81%
Panc1
51%
MiaPaca2
36%
AsPC1
E
Mock
24h H-1PV
48h H-1PV
PI
AnnexinV
B
Cellularity
alive
dead
% of mock
F
Induction of apoptosis
CASP3
PARP1
mock
H-1PV 24h
H-1PV 48h
ratio cleaved to uncleaved form
I
Activation of cathepsins
CTSS
CTSB
nd
mock
H1-PV
ratio cytoplasmic to lysosomal
C
CVS
H-1PV, 50pfu/cell
%of mock
G
gain CVS
AsPC1
MiaPaca2
Panc1
T3M4
%change to H-1PV
+ IM-54
+zVAD
+ 3-MA
+ necrost
+Ac-LVK
H-1PV with inhibitors
J
% of total content
released HMGB1
released LDH
D
rLDH
mock
H1-PV, 50pfu/cell
%of total content
H
gain rLDH
K
H-1PV
mock
total cell count [x10-4]
total HMGB1 content [ng/ml]

pathways. Yet it failed to induce release of any immunogenic determinant besides HMGB1, disproving HMGB1 bias as a consequence of the preferential death modality. Levels of accumulated HMGB1 in PDAC$^{H\text{-}1PV}$ cultures were the same as those recently shown to induce mitochondrial swelling and death in glioblastoma and carcinoma cell lines (66). We thus suspected that released HMGB1 itself might be responsible for ICD-silent killing of PDAC cells. However, added anti-HMGB1 antibodies did not protect PDAC cells from virus-induced death, nor did applied recombinant HMGB1 protein (up to 100 ng/ml) cause their death (data not shown).

HMGB1 release is a death-independent feature of H-1PV infection in PDAC cells. In PDAC$^{H\text{-}1PV}$ cells, HMGB1 release appears to be uncoupled not only from the death modality but also from death/oncolysis in general. The intracellular levels of HMGB1 and LDH are frequently used to monitor cellularity. The leakage of cytoplasmic LDH marks diffusion of the intracellular contents in any case of compromised membrane integrity—apoptotic or necrotic, irreversible or transient (45, 46, 61). Leakage of nuclear HMGB1 is believed to mark only primary necrosis, as an apoptotic process precludes HMGB1 release by enforcing nuclear retention and inclusion in apoptotic bodies (67–70). In PDAC$^{H\text{-}1PV}$ cells, however, the released-to-total-LDH ratio established maximal cumulative leakage in 72-hour cultures at a mean of 30%, while the corresponding value for HMGB1 was 60% and also exceeded LDH indices under apoptotic conditions (Fig. 2J). The linear relationship between the amount of HMGB1 and cellularity, as observed in control PDAC^{mock} setups, was distorted in PDAC$^{H\text{-}1PV}$ cultures, which contained fewer cells (live plus dead; 7 versus 11 $\times$ 10^4) with more total HMGB1 protein (intra- plus extracellular amount; 67 versus 57 ng/ml) (Fig. 2K). The corresponding virus/mock ratios averaged 0.5 $\pm$ 0.1 (cells) and 1.2 $\pm$ 0.1 (HMGB1). With 11 to 73 ng/ml (mean, 42 $\pm$ 13 ng/ml), each PDAC$^{H\text{-}1PV}$ culture contained 3.3 to 9.8 times (mean, 7.1 $\pm$ 1.6 times) more extracellular HMGB1 protein than the 7- $\pm$ 2-ng/ml value expected from LDH release-marked lysis. Furthermore, a depletion of intracellular HMGB1 depots was not observed in infected PDAC cultures (not shown). Overall, the observed HMGB1 overload, distribution, and apoptosis-compatible discharge questioned increased membrane permeability, passive leakage, and oncolysis as the main HMGB1-releasing mechanisms.

Coincidental release of HMGB1 and IL-1β in PDAC$^{H\text{-}1PV}$ cultures. In addition to necrotic release by tumor cells, HMGB1 may be secreted by living immune cells responding to dangerous and inflammatory signals, resulting in a similar alteration of the LDH/HMGB1 pattern (70–72). This cytokine-like production allows HMGB1 to function as an alarmin, i.e., a universal sentinel to viral invasion and double-stranded RNA (dsRNA). Although this route frequently employs an autocrine IL-1β loop, extracellular accumulation of this cytokine in PDAC$^{H\text{-}1PV}$ cultures was detected exclusively in T3M4 supernatants (Fig. 3A), where the IL-1β level rose by 50%. Such a common HMGB1^{++} but selective IL-1β$^{\pm}$ profile indicated that IL-1β secretion may coincide or contribute to but is not a prerequisite for HMGB1 release in PDAC$^{H\text{-}1PV}$ cells.

Detailed analysis showed that T3M4 was the only IL-1β-overexpressing PDAC cell line, with both high basal mRNA levels (1,280 $\pm$ 410 transcripts per 10 kCPB) and constitutive accumulation of the mature IL-1β protein in supernatants (up to 6 pg/ml) 48 h after infection of 2 $\times$ 10^4 cells. In contrast, IL-1β was present at barely detectable levels in other cells (12 $\pm$ 5, 7 $\pm$ 3, and 6 $\pm$ 1 transcripts per 10 kCPB in AsPC1, MiaPaca2, and Panc1 cells, respectively). According to ELISA, the concentration of secreted IL-1β lay at the detection level of 1 pg/ml in Panc1 cells and below that, but above the blank's value, for AsPC1 and MiaPaca2 supernatants (equation-calculated values of approximately 0.15 and 0.3 pg/ml). Without upregulating mRNA expression in any cell line, H-1PV promoted accumulation of extracellular IL-1β protein in T3M4 cells, therefore speaking for a selective activation of the inflammasome/CASP1-containing platform, which is known to enable maturation and release of the leaderless cytokines IL-1β and IL-18, and also HMGB1 (56–58, 70, 73, 74).

Notably, the anti-PDAC chemotherapeutic GEM—recently shown to induce inflammasome-dependent IL-1 release in myeloid suppressor cells (75)—also induced IL-1β production in T3M4 cultures (Fig. 3A). However, GEM failed to trigger HMGB1 release in T3M4 or any other PDAC cell line (Fig. 3B), within the IC_{50} to 100$\times$ IC_{50} range associated with a similar or higher degree of membrane permeability (see Fig. S1A in the supplemental material) and lysis (40 ng/ml) (Fig. 3C) than that with H-1PV. The failure of GEM to elicit an HMGB1 response was in agreement with its proapoptotic activity (see Fig. S1), known to promote nuclear retention of HMGB1 in underacetylated cells (67). The absence of HMGB1 in T3M4^{GEM} supernatants despite similar lysis and a 10 times higher level of IL-1β than that in T3M4$^{H\text{-}1PV}$ cells would be in keeping with the fact that both processes, i.e., apoptosis-compatible leakage and active inflammasome/CASP1-de-

FIG 2 H-1PV-induced PDAC cell death. (A) Infectivity of PDAC cells as determined by immunofluorescence using antibodies targeting the viral nonstructural protein NS1 upon exposure of PDAC cells to H-1PV at an MOI of 10 PFU/cell for 48 h (magnification, ×40). (B) Assessment of cytoreduction at an MOI of 10 PFU/cell by means of crystal violet staining of viable cells (CVS; % of mock) and colorimetric analysis of released LDH as a measure of death (oncolysis). The degree of lysis in the infected cultures was determined by calculating the ratio between released and total (whole Triton X-100-treated cultures) LDH content (rLDH). Subsequent combination of CVS (alive) and LDH (dead) levels allowed us to estimate the total cellularity of each infected culture in relation to the mock setups. (C and D) Cytoreduction (C) and lysis (D) at an MOI of 50 PFU/cell. (E) Compromised membrane integrity (apoptotic and necrotic events) as determined by means of annexin V- and PI-based flow cytometry. The dot blots depict profiles recorded at 24 h for mock infection and at 24 to 48 hpt for H-1PV infection at an MOI of 10 PFU/cell. (F) Molecular markers of apoptosis as assessed by Western blotting of whole-cell lysates, mock or H-1PV treated (10 PFU/cell), using PARP1 and CASP3 antibodies, with results normalized to β-actin levels upon densitometric analyses of images by use of ImageJ software. Data show the ratios between cleaved and uncleaved isoforms. (G and H) Infected PDAC cells (50 PFU/cell) were treated simultaneously with a panel of cell death pathway inhibitors: the oxidative stress inhibitor IM-54, the apoptosis inhibitor Z-VAD-FMK, the autophagy inhibitor 3-MA, the necroptosis inhibitor necrostatin-1, and the cathepsin B inhibitor Ac-LVK-CHO (see Table 1 for details). The data points indicate gain or loss of survival (CVS) and lysis (LDH) between noninhibited H-1PV-infected cultures (as in panels C and D) and inhibited cultures (mean change of value [%]). (I) PDAC cells were infected at an MOI of 10 PFU/cell. At 48 hpt, cells were harvested and samples were subjected to subcellular fractionation. The activities of CTSB and CTSS were determined for cytosolic and crude lysosomal fractions. The ratios between the cytosolic and crude lysosomal values were calculated for mock- and H-1PV-infected cells. nd, not determined. (J) Measurements of released HMGB1 and released LDH differently estimated the degree of oncolysis in infected cultures. (K) The correlation between cellularity and HMGB1 content was observed in mock- but not H-1PV-infected cultures. T, T3M4 cells; P, Panc1 cells; M, MiaPaca2 cells; A, AsPC1 cells.

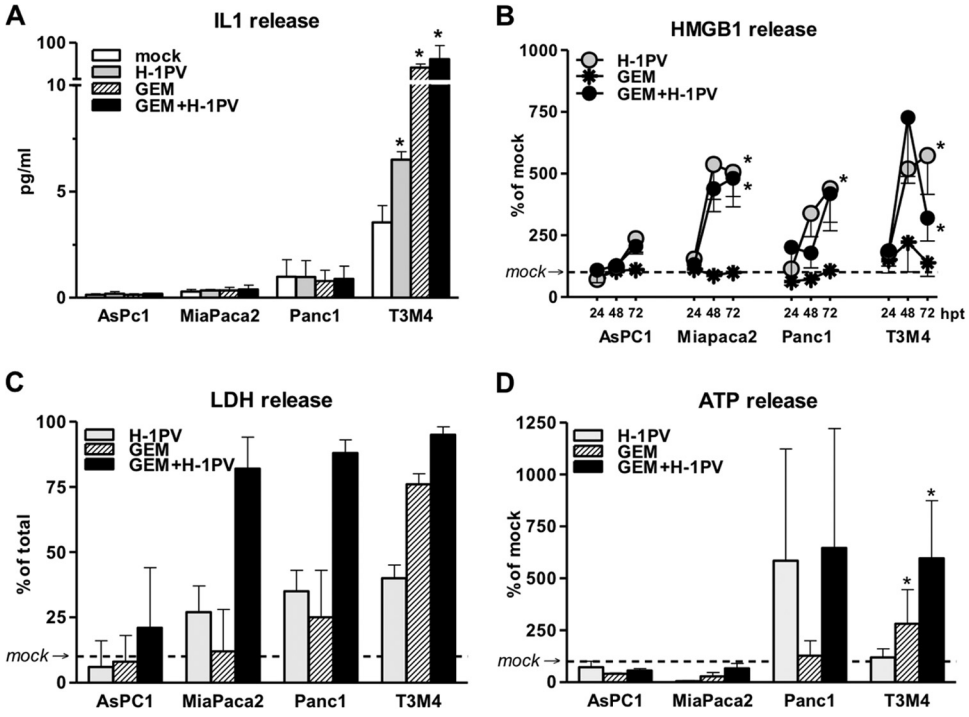

FIG 3 Complementary induction of ICD by gemcitabine (GEM) and H-1PV in PDAC cells. PDAC cultures were treated with H-1PV at an MOI of 10 PFU/cell, with or without previous exposure to GEM for 12 h, at doses ranging from IC_{50} to 100× IC_{50} or 40 ng/ml. The supernatants were harvested between 24 and 72 hpt. (A) Selective secretion of IL-1β in T3M4 cells as determined by commercial ELISA at 48 hpt. (B) Kinetics of HMGB1 released into supernatants. The measurements are presented as percentages of levels detected in mock-infected cultures at each time point (see Fig. 1A for actual levels). (C) Levels of oncolysis in H-1PV-treated cells exposed to 40 ng/ml GEM as detected by LDH release assay at 72 hpt. (D) Selective alteration of extracellular ATP level by GEM (in relation to that in mock-infected cells) at 48 hpt. *, significantly different from mock-treated cultures ($P < 0.05$).

penedent cytoplasmic discharge, require the prior nuclear export of HMGB1 (70, 73).

We concluded that H-1PV-induced release is not a mere reflection of compromised membrane integrity or lysis but an active secretory process. The mechanism by which H-1PV might support the hyperacetylation of DNA or HMGB1 (necessary for nuclear exclusion) (67, 72, 76), in particular, and all stages of secretion, in general, is presently a matter of speculation (see Discussion).

H-1PV keeps the ability to promote HMGB1 release under GEM-imposed apoptotic conditions and complements GEM for induction of the ICD profile. The inability of proapoptotic GEM to induce HMGB1 release might be one of the reasons why this drug fails to provide long-term protection in PDAC patients and might also provide a mechanistic basis for immune system-dependent synergistic effects achieved by combined chemovirotherapy. Therefore, we next examined whether H-1PV was indeed able to overcome the HMGB1 release-blocking activity of GEM. In PDAC cells first treated with GEM and then treated with the virus 10 to 12 h later ($PDAC^{Gem \rightarrow H\text{-}1PV}$ cells), HMGB1 release remained a striking feature of H-1PV infection (Fig. 3B, gray and black circles). This phenomenon coincided with the expression of an apoptotic AnnV-PI phenotype and the activation of the downstream effectors CASP3 and PARP1 (see Fig. S1 in the supplemental material). Notably, the combination of GEM with H-1PV both synergistically promoted oncolysis and kept HMGB1 release at the virus-induced level (Fig. 3B and C). Thus, H-1PV seems not only to trigger release of HMGB1 in PDAC cells undergoing infection-related programmed death but also to override the HMGB1 release blockage imposed by proapoptotic chemotherapeutics.

In PDAC cells, GEM was found to trigger endoplasmic reticulum stress and autophagy (77). We therefore evaluated whether GEM may also trigger release of related ICD determinants. GEM failed to induce CRT translocation in all four PDAC lines tested (data not shown). ATP secretion remained unaltered in AsPC1 and MiaPaca2 cells but was enhanced significantly in T3M4 cells and variably in Panc1 cultures (Fig. 3D). The immunogenic signal of ATP is transmitted by IL-1β being released by immune cells responding to ATP-P2X7 binding by activation of an inflammasome/CASP1 pathway. We observed that constitutive levels of extracellular ATP varied greatly among PDAC cells and correlated inversely with the level of IL-1. Although the GEM-induced level of ATP in T3M4 cells remained lower than the constitutive one in AsPC1 cells, it sufficed to coincide with IL-1 release. These data might question the translational relevance of various ATP levels and their increases in PDAC cells, yet they reveal selective triggering of ICD-relevant pathways by GEM.

Since the HMGB1-releasing effect of H-1PV overcame the HMGB1-blocking effect of GEM, we determined whether the virus acted in a dominant way by also interfering with the GEM-induced ATP release and stronger IL-1β secretion. Upon coexposure, H-1PV did not eliminate or reduce any GEM responses. In contrast, each agent maintained its immunogenic potential without antagonistic or synergistic tendencies: the $PDAC^{GEM}$-specific ATP and IL-1 secretion supplemented $PDAC^{H\text{-}1PV}$-specific HMGB1 and IL-1 release, while the failure of either agent to in-

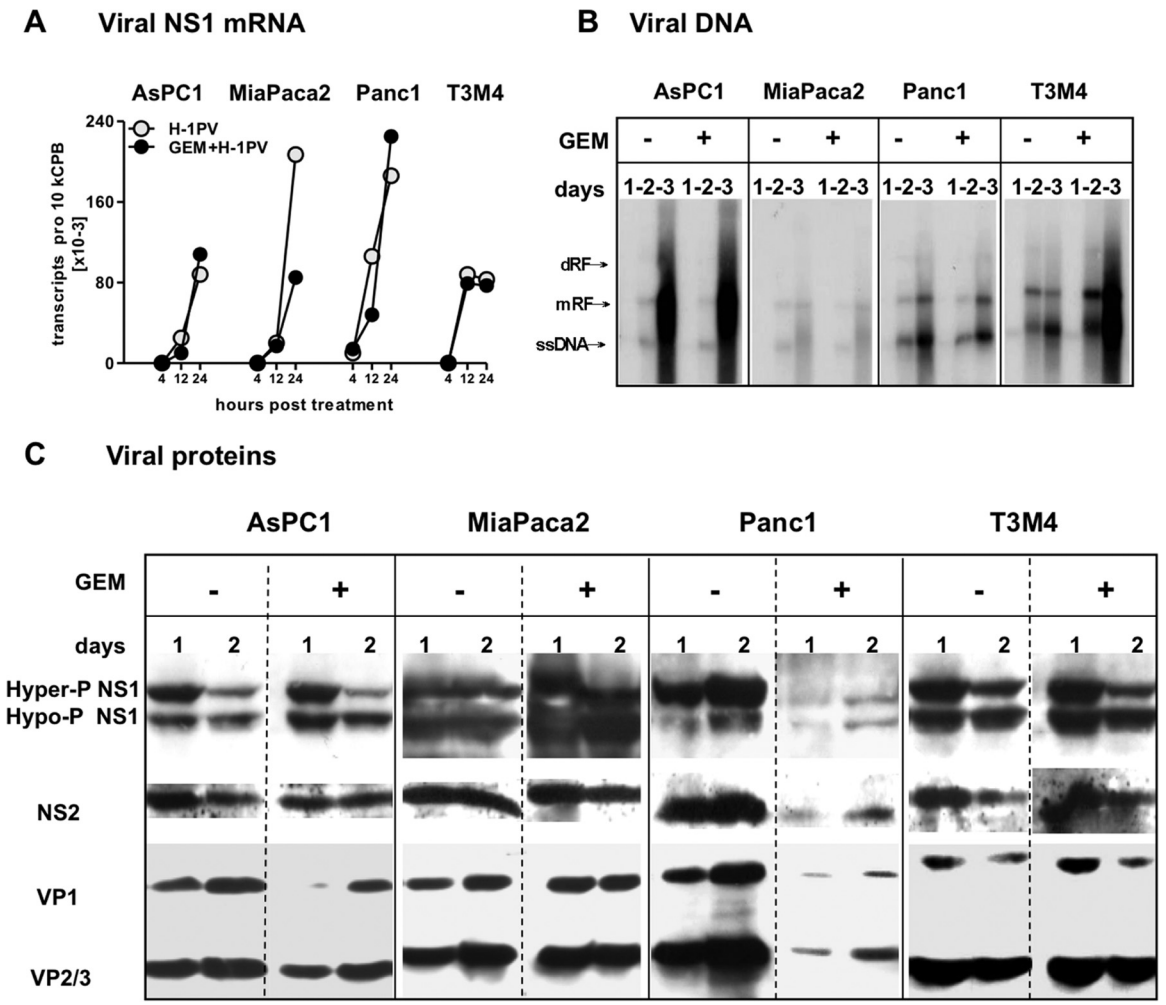

FIG 4 H-1PV replication in GEM-treated PDAC cells. H-1PV was added to PDAC cultures at an MOI of 10 PFU/cell, alone or after 12 hours of preexposure to GEM at the respective IC_{50}s (see Materials and Methods). Cells were harvested at the indicated time points to measure expression of H-1PV determinants (mRNA, DNA, and proteins). (A) At 4 to 24 hpt, the number of NS1 mRNA copies was determined by qRT-PCR, normalized to cyclophilin B levels (10 kCPB), and controlled for vDNA contamination as described in Materials and Methods. (B) Viral DNA replication was assessed by Southern blotting of DNA extracts at 1 to 3 days posttreatment. ssDNA, single-stranded viral DNA genome; mRF, monomer replicative form; dRF, dimer replicative form. (C) Expression of viral proteins NS1 and -2 and VP1 to -3 was analyzed by Western blot analysis of infected cells, using antibodies targeting the respective viral proteins at 1 to 3 days posttreatment.

duce CRT, CD47, and HSP70 exposure was kept after cotreatment (Fig. 3 and data not shown). Thus, the GEM–H-1PV cotreatment promoted cytotoxicity and allowed complementation of the immunogenic profiles triggered by the individual treatments.

H-1PV replication in GEM-treated cells. In view of the absolute dependency of H-1PV replication on the proliferative status of cells, the ability of GEM to reinforce H-1PV cytotoxicity without interfering with the virus-induced HMGB1 release suggested that GEM treatment should be compatible with virus replication—at least until formation of HMGB1-triggering determinants. Indeed, most of the parameters of the viral life cycle were comparable between $PDAC^{H\text{-}1PV}$ and $PDAC^{GEM\rightarrow H\text{-}1PV}$ cultures, except for in Panc1 cells. The GEM-treated Panc1 cells sustained normal levels of viral DNA replication and transcription, but the synthesis of nonstructural (NS1 and NS2) and structural (VP1 and VP2/3) proteins was greatly suppressed (Fig. 4A to C). The overall production of infectious progenies measured at 72 hpt was reduced by GEM cotreatment from 30 to 3 PFU/cell in Panc1 cells and from 6 to 3 PFU/cell in T3M4 cells. Since all infected PDAC cell lines were induced to release HMGB1, these observations suggest that viral DNA or RNA intermediates may serve as triggers of this process. This is in keeping with the view of HMGB1 production as a sentinel reaction to the occurrence of early stages of the viral life cycle, irrespective of cell death.

The onset of the viral life cycle is strictly dependent on the entry of the cells into S phase, with concomitant accumulation of cyclin A1 (CCNA1) (78). Prior to inducing apoptosis, GEM may cause transient arrest in the G_1/S or G_2/M phase of the cell cycle (79–81). According to our data, GEM treatment promoted accumulation of CCNA1 in T3M4 cells within 10 hpt (Fig. 5A and B), peaking at 24 hpt and coinciding with early S arrest (Fig. 5C and D). This effect was kept in cotreated cells and was transient, with CCNA1 levels being normalized and $PDAC^{GEM}$ or $PDAC^{GEM\rightarrow H\text{-}1PV}$ cells progressing to G_2/M at 48 h postinfection. In contrast, treatment with H-1PV alone was not associated with a major CCNA1 induction and led to a cell arrest at the S/G_2 boundary within the first 24

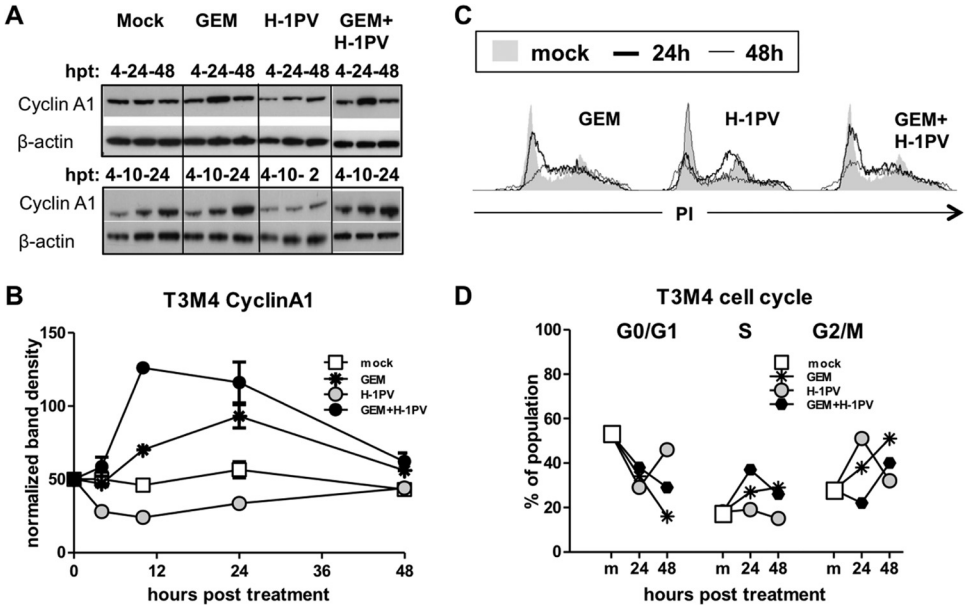

FIG 5 Transient G_1/S block and cyclin A1 overexpression are sufficient to enable compatibility of proliferation-dependent H-1PV with cytotoxic GEM. T3M4 cultures were treated with H-1PV at an MOI of 10 PFU/cell, with or without previous exposure to GEM for 12 h at 40 ng/ml, and analyzed by Western blotting and FACS analysis. (A and B) Kinetics of cyclin A1 protein accumulation as monitored by Western blotting sets comprising 4, 10, and 24 hpt and 4, 24, and 48 hpt. The graph depicts the summarized data obtained by quantification of images by use of ImageJ software. (C and D) Cell cycle analyses were performed by PI staining of the DNA in the treated cells and subsequent FACS-assisted measurement of the fluorescence. Analysis of kinetics revealed transient arrest of the cells by GEM at G_1/S and by H-1PV at the S/G_2 boundary by 24 h (bold lines), with consequent release thereafter (48 h) (thin lines). The proportions of the population in the G_0/G_1, S, and G_2/M cell cycle phases were calculated and plotted to show differences from the mock-treated cells.

hpt, similar to the block observed in stably transfected HEK-293 and HeLa cell lines that express H-1PV NS1 under the control of a tetracycline-inducible promoter (51). At later times, $PDAC^{H\text{-}1PV}$ cells either died or entered mitosis, returning to G_0/G_1 at 48 hpt. Therefore, the GEM treatment resulted in a transient synchronization of cells in a CCNA1-rich S phase, which appeared to support the generation of the viral determinants responsible for HMGB1 induction in cotreated cells.

DISCUSSION

The major aim of our work was to investigate whether parvovirus-induced cell death in PDAC cells is immunogenic, i.e., is associated with the release of three major ICD determinants. Our data showed that H-1PV only promoted the release of HMGB1, and this feature was disassociated from death. None of the other ICD determinants—CRT, ATP, HSP70, uric acid, and CD47—were affected by H-1PV infection. Prevention of CRT exposure in infected cells is considered to be the main effect of many viruses which subvert immunogenicity by precluding uptake by dendritic cells (37). H-1PV failed to induce CRT exposure—an "eat me" signal marking ER stress—in PDAC cells, otherwise responding to MTX (Fig. 1E) but not to doxorubicin (not shown). Whether H-1PV is generally unable to elicit CRT responses remains to be determined.

In contrast, release of HMGB1 was found to alarm the immune system to infectious agents such as hepatitis viruses and HIV (38, 39). HMGB1 can function as a chemoattractant for immune cells, activating them upon binding to TLR2, TLR4, TLR9, and RAGE receptors, thereby initiating an adaptive immune response resulting in engagement of antigen-specific cytotoxic effectors (cytotoxic T lymphocytes [CTLs]) (67, 72, 82, 83). Antitumor protection induced by oncolytic viruses also appears to rely on the release of HMGB1 (41, 43). This is particularly the case for viruses enforced with immunostimulatory elements, as demonstrated by the ability of glycyrrhizin to completely block tumor regression induced by ganciclovir and adenoviral vectors encoding herpes simplex virus 1-thymidine kinase and cytokine Flt3L (Ad-TK+GCV and Ad-Flt3L) in a glioblastoma model (84).

Although the current concept of ICD assumes passive leakage of nonhistone nuclear HMGB1 from postapoptotic/necrotic cells (10), this protein was released by all $PDAC^{H\text{-}1PV}$ cells, whether nondying, necrotic, or succumbing to one of the programmed death pathways, including apoptosis. HMGB1 release was stimulated at levels far higher than those expected from the corresponding LDH values and was not promoted by additional oncolysis upon cotreatment with the proapoptotic drug GEM. This chemotherapeutic alone failed to stimulate HMGB1 release despite strong cytotoxic effects. Loose binding of HMGB1 to the chromatin ensures its rapid leakage from traumatized (necrotic) cells with compromised membrane integrity (67). Apoptosis-specific modifications tighten binding of HMGB1 to underacetylated chromatin and facilitate its disposal within apoptotic bodies, without extracellular leakage. The apoptotic blockade can be overcome by hyperacetylation or exposure of the cells to deacetylase inhibitors, in particular, trichostatin A (TSA) (69–72, 85, 86). Although chromatin-modifying effects of H-1PV have not been described yet, other parvoviruses, such as murine MVMp, canine PV, and rat RPV/UT, have been shown to affect chromatin organization in general, and histone deacetylation in particular (87–89). Alternatively, affinity of HMGB1 for ssDNA and recruitment of HMGB1 to viral structures during replication (90) could interfere with HMGB1 binding to chromatin and facilitate its nuclear exit.

HMGB1 exit from the nucleus may result from lytic replication of H-1PV in infected permissive cells. However, the fact that HMGB1 release is also stimulated by H-1PV in oncolysis-resistant cells (e.g., AsPC1 cells) led us to consider an alternative mechanism, i.e., an active, cytokine-like secretion without loss of viability. According to this view, danger motifs (e.g., lipopolysaccharide [LPS] and dsRNA mimetics) and inflammation (IL-1β and tumor necrosis factor [TNF]) first trigger TSA-like, hyperacetylation-dependent cytoplasmic accumulation of HMGB1. Phosphorylation, redox status, and complexes with DNA appear to influence this process as well (70). The subsequent steps require lysosomal destabilization, inflammasome-dependent activation of CASP1 activity, and an unconventional, ER- and Golgi apparatus-independent mechanism of exocytosis. Similar CASP1 processing and alternative secretion routes are routinely used by cytokines (IL-1, IL-18, and, eventually, IL-33) which lack a signal peptide. IL-1β was found to complex frequently with HMGB1 during release. Cytoplasmic HMGB1 accumulates in secretory lysosomes, whose exocytosis is then triggered by lysophosphatidylcholine (LPC)—a lipid generated by secretory phospholipase A_2 ($sPLA_2$) at inflammatory sites (72, 91–93).

If we assume a cytokine mode of HMGB1 release in PDAC cells, induction of the HMGB1 translocation from the nucleus to the cytoplasm would represent a limiting step, but subsequent steps in the HMGB1 secretory pathway may also be stimulated by infection in $PDAC^{H\text{-}1PV}$ cells. This led us to propose two working hypotheses for the stimulation of cytosolic steps of HMGB1 release: by virions (mechanical model) and by RNA/DNA intermediates (antiviral model).

In the first model, accumulation of incoming virions into endolysosomes may destabilize these organelles, resulting in the release of CTSB without immediate lethal consequences, as documented in the present study. CTSB-triggered assembly of the NRPL3 inflammasome leads to the activation of CASP1, which was found to be overexpressed in PDAC cells (94) and whose potential activation in infected PDAC cells was supported by the release of indicator IL-1β in $T3M4^{H\text{-}1PV}$ cells. The transfer of the viral genome from the endolysosome to the nucleus is thought to involve $sPLA_2$, a cellular mimicry factor displayed by internalized parvoviral capsids (95). Considering the dependence of HMGB1 exocytosis on $sPLA_2$, a viral form of this protein emerges as another attractive candidate to trigger HMGB1 secretion. In addition to $sPLA_2$-induced exocytosis, controlled pore opening during viral trafficking (96), as well as leakage of the cytoplasmic cargo from cells with compromised membrane integrity, might contribute to HMGB1 release.

The second model takes into account the danger signals known to induce cytokine-like HMGB1 secretion. We found that H-1PV-induced HMGB1 release was preserved under conditions of GEM treatment in all four cell lines tested. While production of viral proteins was dramatically reduced by GEM in one of the PDAC cell lines, all four lines cotreated with GEM and H-1PV supported normal levels of viral RNA and DNA synthesis. This result pointed to viral nucleic acids as potential triggers of HMGB1 release, linking this release to the defense system used by host cells to recognize infectious agents' molecular patterns.

The RNA/DNA pattern recognition system, i.e., Toll-like receptors and their partners inducing IFN-α/β and NF-κB-dependent antiviral reactions, was reported to be mobilized in some cells infected with parvoviruses. Lysosomal and cytoplasmic sensors binding viral RNA (TLR3, protein kinase R [PKR], RIG-I, and MAVS) or ssDNA (TLR9) sequences have been shown to respond to infection with the autonomous parvoviruses MVMp and H-1PV (36, 44, 97–100). Notably, the cell-type-dependent pattern of sensor expression determined both induction of the IFN response and permissiveness for virus infection, accounting for the abortion of the viral life cycle in TLR3/TLR9/PKR-positive fibroblasts or immune cells and for the success of virus replication in tumor cells lacking these intracellular receptors. In particular, human immune cells apparently react to an early H-1PV pattern (i.e., input ssDNA via TLR9 receptors) and use IFN-dependent effectors to interrupt the viral life cycle at an early stage (36, 44). In contrast, PDAC cells lack the TLR9 receptor and constitutively fail to develop this early block, allowing the viral life cycle to progress at least to the DNA amplification and transcription stage. It is also known that the ssRNA/dsRNA sensor NLRP3 or the dsDNA sensor AIM2 may activate the inflammasome complex, enabling cytoplasmic autocleavage of CASP1 and resultant release of proinflammatory molecules alarming the immune system (93); their role in parvoviral recognition has not been studied yet.

Theoretically, viral replicative forms (RF) or RNA may serve as ligands of diverse sensors activating HMGB1 and/or IL-1β secretion. In our interpretation, this "delayed" response would allow completion of the viral life cycle up to oncolysis, while efficiently exposing infected PDAC cells to the alerted immune system. This constellation would promote the establishment of an adaptive antitumor immunity concomitant with an antiviral immune response. Cotreatment with GEM might boost the oncolytic component of this process, thus explaining the cooperative effects of combined GEM and H-1PV treatments in preclinical models (32).

Altogether, our data revealed that release of the ICD determinant HMGB1 is a singular, and also common, apoptosis-resistant feature of H-1PV infection of PDAC cells, occurring with or without oncolysis. Instead of being a mere consequence of cell death, HMGB1 release in $PDAC^{H\text{-}1PV}$ cells appears to follow the alternative cytokine secretory pathway. Secreted HMGB1 functions as an alarmin and might represent a general mechanism by which viral infection is signaled to the immune system. In the context of available publications, our data suggest that entering virions and/or synthesis of RNA/DNA intermediates may trigger HMGB1 release. This antiviral mechanism clearly deserves further investigation. The resistance to apoptosis and compatibility of H-1PV-induced HMGB1 secretion with exposure to other ICD-inducing chemotherapeutics warrant the consideration of nonpathogenic H-1PV for inclusion in multimodal anticancer treatments.

ACKNOWLEDGMENTS

This work was supported by DFG grant RA1891/2 to Z. Raykov, by Heidelberger Stiftung Chirurgie and DFG grant GI802/1 to N. A. Giese, and by funds provided by the Institut National de la Santé et de la Recherché Médicale (INSERM) to Unit 701 at DKFZ (Heidelberg, Germany).

We thank Nathalie Salome and Michele Vogel for a gift of antiviral antibodies. We greatly appreciate the technical assistance provided by Monika Meinhardt and Brunhilde Bentzinger (University Hospital Heidelberg) and by Annabel Grewenig and Rita Hörlein (DKFZ).

REFERENCES

1. **Siegel R, Naishadham D, Jemal A.** 2012. Cancer statistics, 2012. CA Cancer J. Clin. **62:**10–29. http://dx.doi.org/10.3322/caac.20138.
2. **Hartwig W, Hackert T, Hinz U, Gluth A, Bergmann F, Strobel O, Buchler MW, Werner J.** 2011. Pancreatic cancer surgery in the new

millennium: better prediction of outcome. Ann. Surg. **254:**311–319. http://dx.doi.org/10.1097/SLA.0b013e31821fd334.
3. **Gillen S, Schuster T, Meyer Zum Buschenfelde C, Friess H, Kleeff J.** 2010. Preoperative/neoadjuvant therapy in pancreatic cancer: a systematic review and meta-analysis of response and resection percentages. PLoS Med. **7:**e1000267. http://dx.doi.org/10.1371/journal.pmed.1000267.
4. **Igney FH, Krammer PH.** 2002. Immune escape of tumors: apoptosis resistance and tumor counterattack. J. Leukoc. Biol. **71:**907–920.
5. **Morse MA, Hall JR, Plate JM.** 2009. Countering tumor-induced immunosuppression during immunotherapy for pancreatic cancer. Expert Opin. Biol. Ther. **9:**331–339. http://dx.doi.org/10.1517/14712590802715756.
6. **Bellone G, Carbone A, Smirne C, Scirelli T, Buffolino A, Novarino A, Stacchini A, Bertetto O, Palestro G, Sorio C, Scarpa A, Emanuelli G, Rodeck U.** 2006. Cooperative induction of a tolerogenic dendritic cell phenotype by cytokines secreted by pancreatic carcinoma cells. J. Immunol. **177:**3448–3460.
7. **Zitvogel L, Kroemer G.** 2009. Anticancer immunochemotherapy using adjuvants with direct cytotoxic effects. J. Clin. Invest. **119:**2127–2130. http://dx.doi.org/10.1172/JCI39991.
8. **Zitvogel L, Apetoh L, Ghiringhelli F, Kroemer G.** 2008. Immunological aspects of cancer chemotherapy. Nat. Rev. Immunol. **8:**59–73. http://dx.doi.org/10.1038/nri2216.
9. **Kepp O, Galluzzi L, Martins I, Schlemmer F, Adjemian S, Michaud M, Sukkurwala AQ, Menger L, Zitvogel L, Kroemer G.** 2011. Molecular determinants of immunogenic cell death elicited by anticancer chemotherapy. Cancer Metastasis Rev. **30:**61–69. http://dx.doi.org/10.1007/s10555-011-9273-4.
10. **Zitvogel L, Kepp O, Kroemer G.** 2011. Immune parameters affecting the efficacy of chemotherapeutic regimens. Nat. Rev. Clin. Oncol. **8:**151–160. http://dx.doi.org/10.1038/nrclinonc.2010.223.
11. **Zappasodi R, Pupa SM, Ghedini GC, Bongarzone I, Magni M, Cabras AD, Colombo MP, Carlo-Stella C, Gianni AM, Di Nicola M.** 2010. Improved clinical outcome in indolent B-cell lymphoma patients vaccinated with autologous tumor cells experiencing immunogenic death. Cancer Res. **70:**9062–9072. http://dx.doi.org/10.1158/0008-5472.CAN-10-1825.
12. **Ciampricotti M, Hau CS, Doornebal CW, Jonkers J, de Visser KE.** 2012. Chemotherapy response of spontaneous mammary tumors is independent of the adaptive immune system. Nat. Med. **18:**344–346. http://dx.doi.org/10.1038/nm.2652.
13. **Michaud M, Martins I, Sukkurwala AQ, Adjemian S, Ma Y, Pellegatti P, Shen S, Kepp O, Scoazec M, Mignot G, Rello-Varona S, Tailler M, Menger L, Vacchelli E, Galluzzi L, Ghiringhelli F, di Virgilio F, Zitvogel L, Kroemer G.** 2011. Autophagy-dependent anticancer immune responses induced by chemotherapeutic agents in mice. Science **334:**1573–1577. http://dx.doi.org/10.1126/science.1208347.
14. **Fucikova J, Kralikova P, Fialova A, Brtnicky T, Rob L, Bartunkova J, Spisek R.** 2011. Human tumor cells killed by anthracyclines induce a tumor-specific immune response. Cancer Res. **71:**4821–4833. http://dx.doi.org/10.1158/0008-5472.CAN-11-0950.
15. **Martins I, Kepp O, Schlemmer F, Adjemian S, Tailler M, Shen S, Michaud M, Menger L, Gdoura A, Tajeddine N, Tesniere A, Zitvogel L, Kroemer G.** 2011. Restoration of the immunogenicity of cisplatin-induced cancer cell death by endoplasmic reticulum stress. Oncogene **30:**1147–1158. http://dx.doi.org/10.1038/onc.2010.500.
16. **Plate JM, Plate AE, Shott S, Bograd S, Harris JE.** 2005. Effect of gemcitabine on immune cells in subjects with adenocarcinoma of the pancreas. Cancer Immunol. Immunother. **54:**915–925. http://dx.doi.org/10.1007/s00262-004-0638-1.
17. **Bellone G, Novarino A, Vizio B, Brondino G, Addeo A, Prati A, Giacobino A, Campra D, Fronda GR, Ciuffreda L.** 2009. Impact of surgery and chemotherapy on cellular immunity in pancreatic carcinoma patients in view of an integration of standard cancer treatment with immunotherapy. Int. J. Oncol. **34:**1701–1715. http://dx.doi.org/10.3892/ijo_00000301.
18. **Bauer C, Bauernfeind F, Sterzik A, Orban M, Schnurr M, Lehr HA, Endres S, Eigler A, Dauer M.** 2007. Dendritic cell-based vaccination combined with gemcitabine increases survival in a murine pancreatic carcinoma model. Gut **56:**1275–1282. http://dx.doi.org/10.1136/gut.2006.108621.
19. **Bauer C, Dauer M, Saraj S, Schnurr M, Bauernfeind F, Sterzik A, Junkmann J, Jakl V, Kiefl R, Oduncu F, Emmerich B, Mayr D, Mussack T, Bruns C, Ruttinger D, Conrad C, Jauch KW, Endres S, Eigler A.** 2011. Dendritic cell-based vaccination of patients with advanced pancreatic carcinoma: results of a pilot study. Cancer Immunol. Immunother. **60:**1097–1107. http://dx.doi.org/10.1007/s00262-011-1023-5.
20. **Dauer M, Herten J, Bauer C, Renner F, Schad K, Schnurr M, Endres S, Eigler A.** 2005. Chemosensitization of pancreatic carcinoma cells to enhance T cell-mediated cytotoxicity induced by tumor lysate-pulsed dendritic cells. J. Immunother. **28:**332–342. http://dx.doi.org/10.1097/01.cji.0000164038.41104.f5.
21. **Ghaneh P, Costello E, Neoptolemos JP.** 2007. Biology and management of pancreatic cancer. Gut **56:**1134–1152. http://dx.doi.org/10.1136/gut.2006.103333.
22. **Wennier S, Li S, McFadden G.** 2011. Oncolytic virotherapy for pancreatic cancer. Expert Rev. Mol. Med. **13:**e18. http://dx.doi.org/10.1017/S1462399411001876.
23. **Cotmore SF, Tattersall P.** 2007. Parvoviral host range and cell entry mechanisms. Adv. Virus Res. **70:**183–232. http://dx.doi.org/10.1016/S0065-3527(07)70005-2.
24. **Giese NA, Raykov Z, DeMartino L, Vecchi A, Sozzani S, Dinsart C, Cornelis JJ, Rommelaere J.** 2002. Suppression of metastatic hemangiosarcoma by a parvovirus MVMp vector transducing the IP-10 chemokine into immunocompetent mice. Cancer Gene Ther. **9:**432–442. http://dx.doi.org/10.1038/sj.cgt.7700457.
25. **Rommelaere J, Geletneky K, Angelova AL, Daeffler L, Dinsart C, Kiprianova I, Schlehofer JR, Raykov Z.** 2010. Oncolytic parvoviruses as cancer therapeutics. Cytokine Growth Factor Rev. **21:**185–195. http://dx.doi.org/10.1016/j.cytogfr.2010.02.011.
26. **Moehler M, Blechacz B, Weiskopf N, Zeidler M, Stremmel W, Rommelaere J, Galle PR, Cornelis JJ.** 2001. Effective infection, apoptotic cell killing and gene transfer of human hepatoma cells but not primary hepatocytes by parvovirus H1 and derived vectors. Cancer Gene Ther. **8:**158–167. http://dx.doi.org/10.1038/sj.cgt.7700288.
27. **Raykov Z, Grekova S, Leuchs B, Aprahamian M, Rommelaere J.** 2008. Arming parvoviruses with CpG motifs to improve their oncosuppressive capacity. Int. J. Cancer **122:**2880–2884. http://dx.doi.org/10.1002/ijc.23472.
28. **Raykov Z, Grekova S, Galabov AS, Balboni G, Koch U, Aprahamian M, Rommelaere J.** 2007. Combined oncolytic and vaccination activities of parvovirus H-1 in a metastatic tumor model. Oncol. Rep. **17:**1493–1499. http://dx.doi.org/10.3892/or.17.6.1493.
29. **Moehler MH, Zeidler M, Wilsberg V, Cornelis JJ, Woelfel T, Rommelaere J, Galle PR, Heike M.** 2005. Parvovirus H-1-induced tumor cell death enhances human immune response in vitro via increased phagocytosis, maturation, and cross-presentation by dendritic cells. Hum. Gene Ther. **16:**996–1005. http://dx.doi.org/10.1089/hum.2005.16.996.
30. **Moehler M, Sieben M, Roth S, Springsguth F, Leuchs B, Zeidler M, Dinsart C, Rommelaere J, Galle PR.** 2011. Activation of the human immune system by chemotherapeutic or targeted agents combined with the oncolytic parvovirus H-1. BMC Cancer **11:**464. http://dx.doi.org/10.1186/1471-2407-11-464.
31. **Grekova SP, Raykov Z, Zawatzky R, Rommelaere J, Koch U.** 2012. Activation of a glioma-specific immune response by oncolytic parvovirus minute virus of mice infection. Cancer Gene Ther. **19:**468–475. http://dx.doi.org/10.1038/cgt.2012.20.
32. **Angelova AL, Aprahamian M, Grekova SP, Hajri A, Leuchs B, Giese NA, Dinsart C, Herrmann A, Balboni G, Rommelaere J, Raykov Z.** 2009. Improvement of gemcitabine-based therapy of pancreatic carcinoma by means of oncolytic parvovirus H-1PV. Clin. Cancer Res. **15:**511–519. http://dx.doi.org/10.1158/1078-0432.CCR-08-1088.
33. **Dempe S, Stroh-Dege AY, Schwarz E, Rommelaere J, Dinsart C.** 2010. SMAD4: a predictive marker of PDAC cell permissiveness for oncolytic infection with parvovirus H-1PV. Int. J. Cancer **126:**2914–2927. http://dx.doi.org/10.1002/ijc.24992.
34. **Bhat R, Dempe S, Dinsart C, Rommelaere J.** 2011. Enhancement of NK cell antitumor responses using an oncolytic parvovirus. Int. J. Cancer **128:**908–919. http://dx.doi.org/10.1002/ijc.25415.
35. **Grekova S, Aprahamian M, Giese N, Schmitt S, Giese T, Falk CS, Daeffler L, Cziepluch C, Rommelaere J, Raykov Z.** 2010. Immune cells participate in the oncosuppressive activity of parvovirus H-1PV and are activated as a result of their abortive infection with this agent. Cancer Biol. Ther. **10:**1280–1289. http://dx.doi.org/10.4161/cbt.10.12.13455.
36. **Grekova SP, Aprahamian M, Daeffler L, Leuchs B, Angelova A, Giese T, Galabov A, Heller A, Giese NA, Rommelaere J, Raykov Z.** 2011.

Interferon gamma improves the vaccination potential of oncolytic parvovirus H-1PV for the treatment of peritoneal carcinomatosis in pancreatic cancer. Cancer Biol. Ther. **12:**888–895. http://dx.doi.org/10.4161/cbt.12.10.17678.
37. **Kepp O, Senovilla L, Galluzzi L, Panaretakis T, Tesniere A, Schlemmer F, Madeo F, Zitvogel L, Kroemer G.** 2009. Viral subversion of immunogenic cell death. Cell Cycle **8:**860–869. http://dx.doi.org/10.4161/cc.8.6.7939.
38. **Jung JH, Park JH, Jee MH, Keum SJ, Cho MS, Yoon SK, Jang SK.** 2011. Hepatitis C virus infection is blocked by HMGB1 released from virus-infected cells. J. Virol. **85:**9359–9368. http://dx.doi.org/10.1128/JVI.00682-11.
39. **Gougeon ML, Melki MT, Saidi H.** 2012. HMGB1, an alarmin promoting HIV dissemination and latency in dendritic cells. Cell Death Differ. **19:**96–106. http://dx.doi.org/10.1038/cdd.2011.134.
40. **Endo Y, Sakai R, Ouchi M, Onimatsu H, Hioki M, Kagawa S, Uno F, Watanabe Y, Urata Y, Tanaka N, Fujiwara T.** 2008. Virus-mediated oncolysis induces danger signal and stimulates cytotoxic T-lymphocyte activity via proteasome activator upregulation. Oncogene **27:**2375–2381. http://dx.doi.org/10.1038/sj.onc.1210884.
41. **Donnelly OG, Errington-Mais F, Steele L, Hadac E, Jennings V, Scott K, Peach H, Phillips RM, Bond J, Pandha H, Harrington K, Vile R, Russell S, Selby P, Melcher AA.** 2013. Measles virus causes immunogenic cell death in human melanoma. Gene Ther. **20:**7–15. http://dx.doi.org/10.1038/gt.2011.205.
42. **Diaconu I, Cerullo V, Hirvinen ML, Escutenaire S, Ugolini M, Pesonen SK, Bramante S, Parviainen S, Kanerva A, Loskog AS, Eliopoulos AG, Pesonen S, Hemminki A.** 2012. Immune response is an important aspect of the antitumor effect produced by a CD40L-encoding oncolytic adenovirus. Cancer Res. **72:**2327–2338. http://dx.doi.org/10.1158/0008-5472.CAN-11-2975.
43. **Huang B, Sikorski R, Kirn DH, Thorne SH.** 2011. Synergistic antitumor effects between oncolytic vaccinia virus and paclitaxel are mediated by the IFN response and HMGB1. Gene Ther. **18:**164–172. http://dx.doi.org/10.1038/gt.2010.121.
44. **Raykov Z, Grekova SP, Horlein R, Leuchs B, Giese T, Giese NA, Rommelaere J, Zawatzky R, Daeffler L.** 2013. TLR-9 contributes to the antiviral innate immune sensing of rodent parvoviruses MVMp and H-1PV by normal human immune cells. PLoS One **8:**e55086. http://dx.doi.org/10.1371/journal.pone.0055086.
45. **Krysko DV, Vanden Berghe T, D'Herde K, Vandenabeele P.** 2008. Apoptosis and necrosis: detection, discrimination and phagocytosis. Methods **44:**205–221. http://dx.doi.org/10.1016/j.ymeth.2007.12.001.
46. **Vanden Berghe T, Grootjans S, Goossens V, Dondelinger Y, Krysko DV, Takahashi N, Vandenabeele P.** 2013. Determination of apoptotic and necrotic cell death in vitro and in vivo. Methods **61:**117–129. http://dx.doi.org/10.1016/j.ymeth.2013.02.011.
47. **Cotmore SF, Tattersall P.** 1988. The NS-1 polypeptide of minute virus of mice is covalently attached to the 5′ termini of duplex replicative-form DNA and progeny single strands. J. Virol. **62:**851–860.
48. **Di Piazza M, Mader C, Geletneky K, Herrero YCM, Weber E, Schlehofer J, Deleu L, Rommelaere J.** 2007. Cytosolic activation of cathepsins mediates parvovirus H-1-induced killing of cisplatin- and TRAIL-resistant glioma cells. J. Virol. **81:**4186–4198. http://dx.doi.org/10.1128/JVI.02601-06.
49. **Chen AY, Qiu J.** 2010. Parvovirus infection-induced cell death and cell cycle arrest. Future Virol. **5:**731–743. http://dx.doi.org/10.2217/fvl.10.56.
50. **Dupressoir T, Vanacker JM, Cornelis JJ, Duponchel N, Rommelaere J.** 1989. Inhibition by parvovirus H-1 of the formation of tumors in nude mice and colonies in vitro by transformed human mammary epithelial cells. Cancer Res. **49:**3203–3208.
51. **Hristov G, Kramer M, Li J, El-Andaloussi N, Mora R, Daeffler L, Zentgraf H, Rommelaere J, Marchini A.** 2010. Through its nonstructural protein NS1, parvovirus H-1 induces apoptosis via accumulation of reactive oxygen species. J. Virol. **84:**5909–5922. http://dx.doi.org/10.1128/JVI.01797-09.
52. **Ran Z, Rayet B, Rommelaere J, Faisst S.** 1999. Parvovirus H-1-induced cell death: influence of intracellular NAD consumption on the regulation of necrosis and apoptosis. Virus Res. **65:**161–174. http://dx.doi.org/10.1016/S0168-1702(99)00115-X.
53. **Rayet B, Lopez-Guerrero JA, Rommelaere J, Dinsart C.** 1998. Induction of programmed cell death by parvovirus H-1 in U937 cells: connection with the tumor necrosis factor alpha signalling pathway. J. Virol. **72:**8893–8903.
54. **Sawai H, Domae N.** 2011. Discrimination between primary necrosis and apoptosis by necrostatin-1 in annexin V-positive/propidium iodide-negative cells. Biochem. Biophys. Res. Commun. **411:**569–573. http://dx.doi.org/10.1016/j.bbrc.2011.06.186.
55. **Kaczmarek A, Vandenabeele P, Krysko DV.** 2013. Necroptosis: the release of damage-associated molecular patterns and its physiological relevance. Immunity **38:**209–223. http://dx.doi.org/10.1016/j.immuni.2013.02.003.
56. **Bergsbaken T, Fink SL, Cookson BT.** 2009. Pyroptosis: host cell death and inflammation. Nat. Rev. Microbiol. **7:**99–109. http://dx.doi.org/10.1038/nrmicro2070.
57. **Fink SL, Cookson BT.** 2005. Apoptosis, pyroptosis, and necrosis: mechanistic description of dead and dying eukaryotic cells. Infect. Immun. **73:**1907–1916. http://dx.doi.org/10.1128/IAI.73.4.1907-1916.2005.
58. **Miao EA, Rajan JV, Aderem A.** 2011. Caspase-1-induced pyroptotic cell death. Immunol. Rev. **243:**206–214. http://dx.doi.org/10.1111/j.1600-065X.2011.01044.x.
59. **Galluzzi L, Kroemer G.** 2008. Necroptosis: a specialized pathway of programmed necrosis. Cell **135:**1161–1163. http://dx.doi.org/10.1016/j.cell.2008.12.004.
60. **Kepp O, Galluzzi L, Zitvogel L, Kroemer G.** 2010. Pyroptosis—a cell death modality of its kind? Eur. J. Immunol. **40:**627–630. http://dx.doi.org/10.1002/eji.200940160.
61. **Chirico WJ.** 2011. Protein release through nonlethal oncotic pores as an alternative nonclassical secretory pathway. BMC Cell Biol. **12:**46. http://dx.doi.org/10.1186/1471-2121-12-46.
62. **Maroto B, Valle N, Saffrich R, Almendral JM.** 2004. Nuclear export of the nonenveloped parvovirus virion is directed by an unordered protein signal exposed on the capsid surface. J. Virol. **78:**10685–10694. http://dx.doi.org/10.1128/JVI.78.19.10685-10694.2004.
63. **Nuesch JP, Rommelaere J.** 2007. A viral adaptor protein modulating casein kinase II activity induces cytopathic effects in permissive cells. Proc. Natl. Acad. Sci. U. S. A. **104:**12482–12487. http://dx.doi.org/10.1073/pnas.0705533104.
64. **Vollmers EM, Tattersall P.** 2013. Distinct host cell fates for human malignant melanoma targeted by oncolytic rodent parvoviruses. Virology **446:**37–48. http://dx.doi.org/10.1016/j.virol.2013.07.013.
65. **Cesen MH, Pegan K, Spes A, Turk B.** 2012. Lysosomal pathways to cell death and their therapeutic applications. Exp. Cell Res. **318:**1245–1251. http://dx.doi.org/10.1016/j.yexcr.2012.03.005.
66. **Gdynia G, Keith M, Kopitz J, Bergmann M, Fassl A, Weber AN, George J, Kees T, Zentgraf HW, Wiestler OD, Schirmacher P, Roth W.** 2010. Danger signaling protein HMGB1 induces a distinct form of cell death accompanied by formation of giant mitochondria. Cancer Res. **70:**8558–8568. http://dx.doi.org/10.1158/0008-5472.CAN-10-0204.
67. **Scaffidi P, Misteli T, Bianchi ME.** 2002. Release of chromatin protein HMGB1 by necrotic cells triggers inflammation. Nature **418:**191–195. http://dx.doi.org/10.1038/nature00858.
68. **Bianchi ME.** 2004. Significant (re)location: how to use chromatin and/or abundant proteins as messages of life and death. Trends Cell Biol. **14:**287–293. http://dx.doi.org/10.1016/j.tcb.2004.04.004.
69. **Muller S, Ronfani L, Bianchi ME.** 2004. Regulated expression and subcellular localization of HMGB1, a chromatin protein with a cytokine function. J. Intern. Med. **255:**332–343. http://dx.doi.org/10.1111/j.1365-2796.2003.01296.x.
70. **Guo ZS, Liu Z, Bartlett DL, Tang D, Lotze MT.** 2013. Life after death: targeting high mobility group box 1 in emergent cancer therapies. Am. J. Cancer Res. **3:**1–20.
71. **Bonaldi T, Talamo F, Scaffidi P, Ferrera D, Porto A, Bachi A, Rubartelli A, Agresti A, Bianchi ME.** 2003. Monocytic cells hyperacetylate chromatin protein HMGB1 to redirect it towards secretion. EMBO J. **22:**5551–5560. http://dx.doi.org/10.1093/emboj/cdg516.
72. **Gardella S, Andrei C, Ferrera D, Lotti LV, Torrisi MR, Bianchi ME, Rubartelli A.** 2002. The nuclear protein HMGB1 is secreted by monocytes via a non-classical, vesicle-mediated secretory pathway. EMBO Rep. **3:**995–1001. http://dx.doi.org/10.1093/embo-reports/kvf198.
73. **Lu B, Nakamura T, Inouye K, Li J, Tang Y, Lundback P, Valdes-Ferrer SI, Olofsson PS, Kalb T, Roth J, Zou Y, Erlandsson-Harris H, Yang H, Ting JP, Wang H, Andersson U, Antoine DJ, Chavan SS, Hotamisligil GS, Tracey KJ.** 2012. Novel role of PKR in inflammasome activation

and HMGB1 release. Nature **488:**670–674. http://dx.doi.org/10.1038/nature11290.
74. **Willingham SB, Allen IC, Bergstralh DT, Brickey WJ, Huang MT, Taxman DJ, Duncan JA, Ting JP.** 2009. NLRP3 (NALP3, cryopyrin) facilitates in vivo caspase-1 activation, necrosis, and HMGB1 release via inflammasome-dependent and -independent pathways. J. Immunol. **183:**2008–2015. http://dx.doi.org/10.4049/jimmunol.0900138.
75. **Bruchard M, Mignot G, Derangere V, Chalmin F, Chevriaux A, Vegran F, Boireau W, Simon B, Ryffel B, Connat JL, Kanellopoulos J, Martin F, Rebe C, Apetoh L, Ghiringhelli F.** 2013. Chemotherapy-triggered cathepsin B release in myeloid-derived suppressor cells activates the Nlrp3 inflammasome and promotes tumor growth. Nat. Med. **19:**57–64. http://dx.doi.org/10.1038/nm.2999.
76. **Evankovich J, Cho SW, Zhang R, Cardinal J, Dhupar R, Zhang L, Klune JR, Zlotnicki J, Billiar T, Tsung A.** 2010. High mobility group box 1 release from hepatocytes during ischemia and reperfusion injury is mediated by decreased histone deacetylase activity. J. Biol. Chem. **285:**39888–39897. http://dx.doi.org/10.1074/jbc.M110.128348.
77. **Donadelli M, Dando I, Zaniboni T, Costanzo C, Dalla Pozza E, Scupoli MT, Scarpa A, Zappavigna S, Marra M, Abbruzzese A, Bifulco M, Caraglia M, Palmieri M.** 2011. Gemcitabine/cannabinoid combination triggers autophagy in pancreatic cancer cells through a ROS-mediated mechanism. Cell Death Dis. **2:**e152. http://dx.doi.org/10.1038/cddis.2011.36.
78. **Bashir T, Horlein R, Rommelaere J, Willwand K.** 2000. Cyclin A activates the DNA polymerase delta-dependent elongation machinery in vitro: a parvovirus DNA replication model. Proc. Natl. Acad. Sci. U. S. A. **97:**5522–5527. http://dx.doi.org/10.1073/pnas.090485297.
79. **Cappella P, Tomasoni D, Faretta M, Lupi M, Montalenti F, Viale F, Banzato F, D'Incalci M, Ubezio P.** 2001. Cell cycle effects of gemcitabine. Int. J. Cancer **93:**401–408. http://dx.doi.org/10.1002/ijc.1351.
80. **Azzariti A, Bocci G, Porcelli L, Fioravanti A, Sini P, Simone GM, Quatrale AE, Chiarappa P, Mangia A, Sebastian S, Del Bufalo D, Del Tacca M, Paradiso A.** 2011. Aurora B kinase inhibitor AZD1152: determinants of action and ability to enhance chemotherapeutics effectiveness in pancreatic and colon cancer. Br. J. Cancer **104:**769–780. http://dx.doi.org/10.1038/bjc.2011.21.
81. **Pauwels B, Korst AE, Pattyn GG, Lambrechts HA, Van Bockstaele DR, Vermeulen K, Lenjou M, de Pooter CM, Vermorken JB, Lardon F.** 2003. Cell cycle effect of gemcitabine and its role in the radiosensitizing mechanism in vitro. Int. J. Radiat. Oncol. Biol. Phys. **57:**1075–1083. http://dx.doi.org/10.1016/S0360-3016(03)01443-3.
82. **Apetoh L, Ghiringhelli F, Tesniere A, Criollo A, Ortiz C, Lidereau R, Mariette C, Chaput N, Mira JP, Delaloge S, Andre F, Tursz T, Kroemer G, Zitvogel L.** 2007. The interaction between HMGB1 and TLR4 dictates the outcome of anticancer chemotherapy and radiotherapy. Immunol. Rev. **220:**47–59. http://dx.doi.org/10.1111/j.1600-065X.2007.00573.x.
83. **Sims GP, Rowe DC, Rietdijk ST, Herbst R, Coyle AJ.** 2010. HMGB1 and RAGE in inflammation and cancer. Annu. Rev. Immunol. **28:**367–388. http://dx.doi.org/10.1146/annurev.immunol.021908.132603.
84. **Candolfi M, Yagiz K, Foulad D, Alzadeh GE, Tesarfreund M, Muhammad AK, Puntel M, Kroeger KM, Liu C, Lee S, Curtin JF, King GD, Lerner J, Sato K, Mineharu Y, Xiong W, Lowenstein PR, Castro MG.** 2009. Release of HMGB1 in response to proapoptotic glioma killing strategies: efficacy and neurotoxicity. Clin. Cancer Res. **15:**4401–4414. http://dx.doi.org/10.1158/1078-0432.CCR-09-0155.
85. **Bell CW, Jiang W, Reich CF, 3rd, Pisetsky DS.** 2006. The extracellular release of HMGB1 during apoptotic cell death. Am. J. Physiol. Cell Physiol. **291:**C1318–C1325. http://dx.doi.org/10.1152/ajpcell.00616.2005.
86. **Dong Xda E, Ito N, Lotze MT, Demarco RA, Popovic P, Shand SH, Watkins S, Winikoff S, Brown CK, Bartlett DL, Zeh HJ, 3rd.** 2007. High mobility group box I (HMGB1) release from tumor cells after treatment: implications for development of targeted chemoimmunotherapy. J. Immunother. **30:**596–606. http://dx.doi.org/10.1097/CJI.0b013e31804efc76.
87. **Ihalainen TO, Niskanen EA, Jylhava J, Paloheimo O, Dross N, Smolander H, Langowski J, Timonen J, Vihinen-Ranta M.** 2009. Parvovirus induced alterations in nuclear architecture and dynamics. PLoS One **4:**e5948. http://dx.doi.org/10.1371/journal.pone.0005948.
88. **Iseki H, Shimizukawa R, Sugiyama F, Kunita S, Iwama A, Onodera M, Nakauchi H, Yagami K.** 2005. Parvovirus nonstructural proteins induce an epigenetic modification through histone acetylation in host genes and revert tumor malignancy to benignancy. J. Virol. **79:**8886–8893. http://dx.doi.org/10.1128/JVI.79.14.8886-8893.2005.
89. **Op De Beeck A, Caillet-Fauquet P.** 1997. The NS1 protein of the autonomous parvovirus minute virus of mice blocks cellular DNA replication: a consequence of lesions to the chromatin? J. Virol. **71:**5323–5329.
90. **Cotmore SF, Christensen J, Tattersall P.** 2000. Two widely spaced initiator binding sites create an HMG1-dependent parvovirus rolling-hairpin replication origin. J. Virol. **74:**1332–1341. http://dx.doi.org/10.1128/JVI.74.3.1332-1341.2000.
91. **Sollberger G, Strittmatter GE, Garstkiewicz M, Sand J, Beer HD.** 2014. Caspase-1: the inflammasome and beyond. Innate Immun. **20:**115–125. http://dx.doi.org/10.1177/1753425913484374.
92. **Denes A, Lopez-Castejon G, Brough D.** 2012. Caspase-1: is IL-1 just the tip of the ICEberg? Cell Death Dis. **3:**e338. http://dx.doi.org/10.1038/cddis.2012.86.
93. **Hornung V, Latz E.** 2010. Intracellular DNA recognition. Nat. Rev. Immunol. **10:**123–130. http://dx.doi.org/10.1038/nri2690.
94. **Gansauge S, Gansauge F, Yang Y, Muller J, Seufferlein T, Ramadani M, Beger HG.** 1998. Interleukin 1beta-converting enzyme (caspase-1) is overexpressed in adenocarcinoma of the pancreas. Cancer Res. **58:**2703–2706.
95. **Zadori Z, Szelei J, Lacoste MC, Li Y, Gariepy S, Raymond P, Allaire M, Nabi IR, Tijssen P.** 2001. A viral phospholipase A2 is required for parvovirus infectivity. Dev. Cell **1:**291–302. http://dx.doi.org/10.1016/S1534-5807(01)00031-4.
96. **Bar S, Daeffler L, Rommelaere J, Nuesch JP.** 2008. Vesicular egress of non-enveloped lytic parvoviruses depends on gelsolin functioning. PLoS Pathog. **4:**e1000126. http://dx.doi.org/10.1371/journal.ppat.1000126.
97. **Ventoso I, Berlanga JJ, Almendral JM.** 2010. Translation control by protein kinase R restricts minute virus of mice infection: role in parvovirus oncolysis. J. Virol. **84:**5043–5051. http://dx.doi.org/10.1128/JVI.02188-09.
98. **Sieben M, Schafer P, Dinsart C, Galle PR, Moehler M.** 2013. Activation of the human immune system via Toll-like receptors by the oncolytic parvovirus H-1. Int. J. Cancer **132:**2548–2556. http://dx.doi.org/10.1002/ijc.27938.
99. **Mattei LM, Cotmore SF, Tattersall P, Iwasaki A.** 2013. Parvovirus evades interferon-dependent viral control in primary mouse embryonic fibroblasts. Virology **442:**20–27. http://dx.doi.org/10.1016/j.virol.2013.03.020.
100. **Mattei LM, Cotmore SF, Li L, Tattersall P, Iwasaki A.** 2013. Toll-like receptor 9 in plasmacytoid dendritic cells fails to detect parvoviruses. J. Virol. **87:**3605–3608. http://dx.doi.org/10.1128/JVI.03155-12.